PROGRESSION OF SYMPTOMS AND DIFFERENCES IN THE RESPONSE OF DIFFERENT SKELETAL MUSCLES TO THE M1592V MUTATION OF $Na_{V1.4}$ THAT CAUSES HYPERKALEMIC PERIODIC PARALYSIS

By

Shiemaa Khogali

Thesis submitted to the

Faculty of Graduate and Postdoctoral Studies

in partial fulfillment of the requirements for the degree of

Masters of Science

Cellular and Molecular Medicine

Faculty of Medicine

University of Ottawa

ABSTRACT

Hyperkalemic periodic paralysis is characterized by myotonic discharges followed by paralysis. Caused by a mutation in the gene encoding for $Na_{V1.4}$ channel, patients do not experience symptoms during infancy, but the onset starts between 1-10 years of age. The symptoms severity then increases with age until adolescence. A large increase in gene expression marked by an increase in oxidative capacity of muscles has also been reported in HyperKPP. It is possible that the onset of symptoms is related solely to $Na_{V1.4}$ channel content/activity reaching a critical level. It is also possible that the onset of some symptoms are due to defective $Na_{V1.4}$, while other symptoms and the increase in severity with age are related to changes in membrane components as a result of changes in gene expression. To test these possibilities, the progression of paralysis and changes in fiber types were followed with age in HyperKPP mice in relation to changes in $Na_{V1.4}$ content and activity. Changes in fiber types (index of changes in gene expression), started after the onset of paralysis was observed, which coincided with $Na_{V1.4}$ channels reaching maximum expression. Therefore, the onset of symptoms was related to defective $Na_{V1.4}$ channels.

TABLE OF CONTENTS

LIST OF TABLES

LIST OF FIGURES

LIST OF ABBREVIATIONS

AP: Action potential

Na^+: Sodium ion

K^+: Potassium ion

Ca^{2+}: Calcium ion

Cl^-: Chloride ion

HyperKPP: Hyperkalemic periodic paralysis

$Mouse^{(+/M1592V)}$: Hyperkalemic periodic paralysis mouse model with M1592V mutation

W.T.: Wild type

$Na_{V1.4}$: Skeletal muscle voltage-gated Na^+ channel (adult skeletal)

$Na_{V1.5}$: Cardiac muscle voltage-gated Na^+ channel (embryonic skeletal)

K_V: Voltage-gated K^+ channel

SR: sarcoplasmic reticulum

ATP: Adenosine triphosphate

E_m: membrane potential

$Kir_{2.1}$: strong inward rectifier K^+ channel

K_{ATP}: ATP-sensitive K^+ channel

ClC-1: Chloride channel 1

E_{Na}: Equilibrium potential of Na^+

PAM: Potassium aggravated myotonia

PMC: Paramyotonia congenita

HypoKPP: Hypokalemic periodic paralysis

HEK293: Human embryonic kidney cells line 293

rSkM1: rat skeletal Na^+ channel

hH1a: Human cardiac Na^+ channel

I-V: current-voltage relationship

G-V: Conductance-voltage relationship

MHC: Myosin heavy chain

CLFS: Chronic low frequency stimulation

NFAT: Nuclear factor for activated T cells

MEF2: Myocyte enhancer factor 2

PGC-1α: Peroxisome-proliferator-activated receptor-gamma coactivator-1α

EDL: Extensor digitorum longus

FDB: Flexor digitorum brevis

TA: Tibialis anterior

I_{Na}: Na^+ current

ACKNOWLEDGEMENTS

First, I would like to thank my supervisor and mentor Dr. Jean-Marc Renaud. I consider myself lucky to be a student in his laboratory. His dedication to his work and students were inspiring, and his support every step of the way was the reason behind accomplishing my goal of completing this Masters degree. I also would like to thank my advisory committee, Dr. William Staines and Dr. Pierre Fortier for their valuable advice and guidance.

A big thank you to CMM technical staff, especially Kim Wong For her support though out my M.Sc. years. And another big thank you to my past and present laboratory colleagues.

I owe huge thanks to my wonderful family, for all the support and encouragement I received through out my entire life. Your belief in education drives me to strive for more. And finally a very special thank you to my husband and best friend, Ward, for putting up with me and providing me with strength and support. To you, mama, baba, and Ward I dedicate this thesis.

CHAPTER 1

INTRODUCTION

Muscle contraction is an event initiated by action potentials (AP), which consist of a depolarization phase governed by Na^+ influx into the muscle fiber, followed by a repolarization phase governed by K^+ efflux. The electrochemical balance across the cell membrane for Na^+, K^+, Cl^- and Ca^{2+} is regulated by ion channels and transporters, which in turn regulate resting membrane potential (E_m) and excitability of muscle fibers.

Hyperkalemic periodic paralysis (HyperKPP) is a complex channelopathy caused by one of nine different missense mutations in the SCN4A gene encoding for the skeletal muscle voltage-gated Na^+ channel, $Na_{V1.4}$. The defect in $Na_{V1.4}$ channels causes a persistent Na^+ influx leading to myotonic discharges followed by complete paralysis.[1, 2] The paralysis usually affects limb muscles while sparing respiratory muscles such as the diaphragm.[3-6] HyperKPP muscles were also found to have increased oxidative capacity and changes in fiber types, indicating changes at the level of gene expression.[4, 7]

An interesting feature of the disease prognosis is the absence of symptoms during infancy despite carrying the mutation. However, once the symptoms start, they increase in severity and frequency with age peaking at adolescence. An explanation to this feature can be related either to the $Na_{V1.4}$ channel content, reaching a critical level that gives rise to the symptoms, or to changes in expression of other channels caused by changes in gene expression.

The symptoms tend to regress after the age of 30, but replaced by severe myopathy, which

debilitates patients and reduces their quality of life. In some extreme cases patients may become wheelchair-bound.[5, 6]

The major focus of this project was to investigate the degree to which $Na_{V1.4}$ channel content and/or activity contribute to the HyperKPP symptoms with age. To fulfill that, a large study was undertaken to follow the progression of symptoms with age in relation to $Na_{V1.4}$ channel content and activity. While, some studies involved testing muscles *in vitro*, this study's overall objective was to determine the progression of symptoms *in vivo*. The *in vivo* characterization of HyperKPP in this study involved monitoring the occurrence of paralysis, exercise capacity of HyperKPP mice, changes in myosin isoforms expression used as an index of changes in gene expression, and finally fiber damage in HyperKPP. A HyperKPP mouse model was used for this project. This mouse was generated by knocking in a mutation in its genome that was equivalent to one of the human HyperKPP mutations. This mutation was M1592V, and the mouse model would be referred to as Mouse$^{(+/M1592V)}$ for the reminder of this thesis.[7]

FROM ACTION POTENTIAL TO CONTRACTION

Action potential (AP) is the first step that ultimately leads to muscle contraction. It is an event at which E_m rapidly depolarizes from −80 mV to +30 mV following a stimulus and repolarizes back to −80 mV.[8] The depolarization is caused by an alteration in the permeability of membrane to Na^+ ions.

A motor neuron stimulates a muscle fiber by releasing acetylcholine neurotransmitter (ACh) at the neuromuscular junction (NMJ). Upon binding to its receptors on the endplate, a larger depolarization occurs due to Na^+ influx. When E_m reaches −60 mV, which is the threshold for activating $Na_{V1.4}$ channels, AP is triggered allowing more Na^+ influx and

further depolarization. This causes the rising phase of the AP until the membrane potential reaches +30 mV. At that voltage, $Na_{V1.4}$ channels inactivate, and voltage-gated K^+ channels (K_V) open allowing K^+ to escape to the extracellular fluid. Both events lead to repolarization of E_m and cause the falling phase of AP.

AP propagates from the NMJ along the cell membrane and the t-tubules of skeletal muscles, where the depolarization activates Ca^{2+} release from the sarcoplasmic reticulum (SR) into the cytosol. In order to expose the myosin binding site on actin, Ca^{2+} binds to troponin to displace tropomyosin from the active binding site. This allows for actin-myosin cross-bridge formation, leading to muscle contraction utilizing the necessary adenosine triphosphate (ATP).[9]

ION CHANNELS

Ion channels are crucial membrane proteins in living cells that allow the passage of ions such as Na^+, K^+, Cl^-, and Ca^{2+} from one side of the excitable membrane to the other. These ions and their channels play major roles in the regulation of AP, as well as maintaining membrane excitability.[8]

Ion channels controlling membrane potential (E_m) in skeletal muscle

The distribution of ions on either side of the membrane creates a diffusion gradient. When ions are permeable, they create currents, which set specific membrane potentials. At rest, E_m of skeletal muscles is around −80 mV.[8] There are three major channels responsible for resting E_m. The first channel, responsible for 70-80% of membrane conductance at rest is the voltage-gated Cl^- channel (ClC-1) and is located mainly in t-tubules[10]. The second and third channels that are activated at rest are K^+ channels: the strong inward rectifier K^+

channel ($Kir_{2.1}$), and the ATP-sensitive K^+ channel (K_{ATP}).[11-13]

During AP, $Na_{V1.4}$ channels become the main channels controlling E_m causing the rising phase of AP to +30 mV, and then K_V channels take over to repolarize the membrane back to resting potentials. Inward rectifiers $Kir_{2.1}$ channels are also important when $[K^+]_e$ increases, such as during prolonged muscle activation, to facilitate the re-uptake of K^+.[9, 14]

Channelopathies

Any defect or alteration in the function or expression of any ion channel results in what is known as channelopathies (Fig. 1-1), which affect the generation and propagation of APs and ultimately alter the membrane excitability and muscle contraction. Channelopathies are caused by mutations in the gene encoding for an ion channel altering the functionality of the channel. The outcome of these mutations are diseases with symptoms ranging between two extremes: myotonia, defined as the repetitive firing of action potentials, and paralysis, which is the complete absence of electrical activity even when stimulated leading to loss of muscle excitability (Fig. 1-1). Myotonia congenita and potassium aggravated myotonia (PAM) caused by mutations in the ClC-1 and $Na_{V1.4}$ channels, respectively, are two channelopathies for which myotonia is the only symptom. At the other extreme, channelopathies that only present paralysis are Anderson-Tawil syndrome, which result from mutations in the $Kir_{2.1}$ channels, and hypokalemic periodic paralysis (HypoKPP), which results from mutations of either $Ca_{V1.1}$ or $Na_{V1.4}$.[15, 16] Interestingly, other mutations in the $Na_{V1.4}$ channel result in channelopathies that are characterized by both myotonia and paralysis, as in paramyotonia congenita (PMC) and hyperkalemic periodic paralysis (HyperKPP), the latter being the focus of this research project.

Hyperkalemic periodic paralysis (HyperKPP)

HyperKPP is a rare* autosomal dominant muscle disorder with complete or nearly complete penetrance that affect humans and horses.[3] It is characterized by myotonic discharges, accompanied by elevated serum K^+ levels from the normal 4 mM up to 8 mM. The myotonic discharges are usually followed by complete paralysis that mainly affects the limb muscles while sparing face, ocular and respiratory muscles despite the expression of $Na_{V1.4}$ at least in the diaphragm, a major respiratory muscle.[17] However, homozygote horses have a more severe condition with cardiac and respiratory distress.[3, 4, 18] In many cases the paralysis completely immobilized patients and they were often bed-confined for a period of time ranging from few hours to days.[5, 6]

Paralytic attacks can be triggered by various stimuli. The two most consistent triggers are ingestion of K^+ salts (trigger symptoms 100% of the times) and rest after strenuous exercise (80%). Other triggers such as exposure to cold (54%), emotional stress (34%), and fasting (25%) were reported to be less consistent triggers of symptoms.[5]

Symptoms of HyperKPP could be relatively managed using various drugs to reduce the severity and frequency of paralytic attacks. Calcium gluconate, for example, partially alleviates the severity of attacks, while acetazolamide reduces the frequency of attacks.[3, 19] Other treatments include inhalation of β-adrenergic agonists, and thiazide diuretics.[20] Another treatment used to prevent the paralysis is mild exercise such as walking. Unfortunately, some of these treatments become ineffective over time and none of their mechanism of action is fully understood.[21, 22]

* Prevalence 1:200,000[11]

FIGURE 1-1

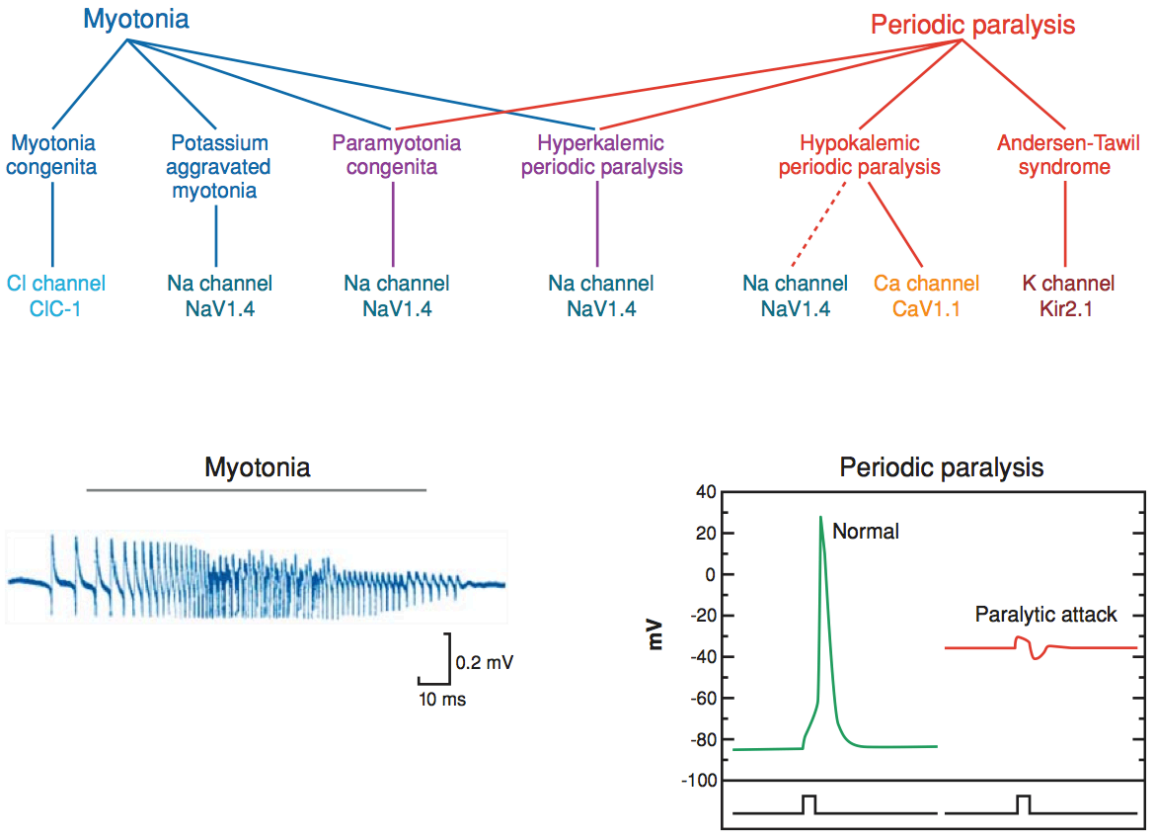

Figure 1-1: Clinical spectrum of nondystrophic myotonias and periodic paralyses. Myotonia predominates in disorders further to the left in this spectrum, whereas periodic paralysis is the major symptom for those toward the right. The underlying molecular genetic defects in each of these disorders are mutations in voltage-gated ion channel genes (*middle row*). Insets below show an electromyographic recording of a myotonic burst (*left*), computer simulations of an action potential in normal muscle (*right*), and depolarization-induced loss of excitability during an attack of periodic paralysis (*right*). *(Figure and legend taken from Cannon, 2006)*[15]

Due to the fact that HyperKPP is caused by a mutation in the SCN4A gene encoding for $Na_{V1.4}$ channel, it is important to understand the family, structure, characteristics and functions of the $Na_{V1.4}$ channel. Therefore, the next two sections will review i) $Na_{V1.4}$ channels, and ii) the physiological response to HyperKPP mutations.

Na_V CHANNELS

Family of Na^+ channels

$Na_{V1.4}$ channel consists of two subunits: (1) the α-subunit, which is the largest and the pore-forming subunit, and (2) the smaller and regulatory β-subunit (Fig. 1-2).

The α-subunits of Na_V channels are large and complex glycoproteins. There are nine mammalian α-subunit isoforms in Na_V channels that have been identified in different tissues (Table 1-1).[23] $Na_{V1.4}$ is the only adult voltage-gated Na^+ channel expressed in adult skeletal muscles including the diaphragm, while $Na_{V1.5}$ is expressed in cardiac muscle as well as in embryonic skeletal muscle. Other Na_V isoforms are expressed in different neurons in the CNS and PNS as seen in Table 1-1. This is the reason why cardiac and neuronal functions are not affected in HyperKPP, however, rare cardiac arrest cases in HyperKPP occurred as a result of steep increases in plasma K^+ that accompanies the paralysis.[24]

Molecular structure of Na_V channels

The α-subunit is composed of 4 domains (I-IV) that are highly conserved among all known Na^+ channels, as well as most cation-selective voltage-dependent channels such as Ca^{2+} and K^+ channels.[25-27] Each domain consists of six transmembrane segments (S1-S6) as seen in Figure 1-2. [28] The first three segments (S1, S2, S3) have some charged amino acids and are weakly amphipathic, while the S4 segment of each domain consists of 4-8 positively

charged amino acids (Lysines or Arginines) at every third position. The two remaining segments (S5 and S6) have no charged amino acids and are the pore-forming segments.[27]

The β-subunit is a small glycoprotein consisting of a single transmembrane segment, an extracellular N-terminus, and an intracellular C-terminus (Fig. 1-2).[27]

Studies have shown that the expression of the α-subunit alone is sufficient to form a functional Na^+ channel. Ji et al[29] recorded Na^+ currents from two *Xenopus* oocytes: one that expressed only the α-subunit, and the other co-expressed both α and β subunits. Channels activated when the oocyte was depolarized to −10 mV from a holding potential of −90 mV, but then slowly inactivated in oocytes when only the α-subunit was expressed. The co-expression of α and β subunits in these oocytes restored the rapid inactivation of the normal channels.

Electrophysiological characteristics of Na_V channels

Voltage-gated Na^+ channels are regulated by three processes, each with its own gating mechanism, in response to changes in membrane potential: activation, fast inactivation, and slow inactivation.

Activation. Under steady-state conditions, the current-voltage (I-V) curve shows the activation threshold for skeletal $Na_{V1.4}$ channels to be at around −60 mV, while at E_m more negative than −60 mV, $Na_{V1.4}$ channels are closed (Fig. 1-3A). Peak Na^+ current (I_{Na}) occurs at −30 to −20 mV, as more channels are open at that potential. In Figure 1-3A, I_{Na} does not decrease to zero because the channel closes, but because E_m approaches the equilibrium potential for Na^+ (E_{Na}), at which the rates of Na^+ influx and efflux are equal, and therefore no net I_{Na} is measured. In fact, as shown in Figure 1-3B, maximum Na^+ channel conductance occurs at −20 mV, when all channels are open. These parameters were established in several

studies using voltage-clamp techniques in *Xenopus oocytes* and HEK293 cell line. Figure 1-3 compares rat skeletal $Na_{V1.4}$ (rSkM1) and human cardiac $Na_{V1.5}$ channels (hH1a). Generally, in cardiac channels there was a shift in peak I_{Na} and G_{max} towards hyperpolarized potentials, indicating that these channels activate at more negative potentials compared to skeletal muscle $Na_{V1.4}$ channels.[30]

Fast inactivation occurs within 1-2 milliseconds of depolarization to terminate the influx of Na^+ during AP and facilitate repolarization.[31] When a channel is inactivated, it does not respond to further stimulation and remains inactivated. Under steady-state conditions, normal $Na_{V1.4}$ channels start to fast inactivate at −80 mV. At −40 mV, 100% of Na^+ channels are fast-inactivated (Fig. 1-4).[32, 33] AP occurs as a result of the overlap between activation and fast inactivation. The activation gate responds immediately upon depolarization, whereas the inactivation process has a slightly delayed response to depolarization (1-2 millisecods).

Slow inactivation occurs after a prolonged depolarization (60-90 seconds), unlike the brief depolarization required for fast inactivation.[34] This process is believed to regulate the excitability of the membrane (decreasing Na^+ current amplitude) by modulating the availability of Na^+ channels for AP under prolonged depolarizations. Under steady-state conditions, there is no slow inactivation of $Na_{V1.4}$ channels at voltages more negative than −100 mV. Slow inactivation starts at −100 to −90 mV and is completed by −20 mV at which almost all of Na^+ channels are slow-inactivated (100% steady-state slow inactivation was not attained under most experimental conditions) (Fig. 1-5). [33-35]

TABLE 1-1

Type	Former Name	Gene symbol	Chromosome location	Primary tissue
$Na_{V1.1}$	rat I HBSCI GPBI SCN1A	SCN1A	Mouse 2 Human 2q24	CNS PNS
$Na_{V1.2}$	rat II HBSCII HBA	SCN2A	Mouse 2 Human 2q23-24	CNS
$Na_{V1.3}$	rat III	SCN3A	Mouse 2 Human 2q24	CNS
$Na_{V1.4}$	SkM1, μ1	SCN4A	Mouse 11 Human 17q23-25	sk. Muscle
$Na_{V1.5}$	SkM2 H1	SCN5A	Mouse 9 Human 3p21	Uninnervated sk. Muscle, heart
$Na_{V1.6}$	NaCh6 PN4 Scn8a CerIII	SCN8A	Mouse 15 Human 12q13	CNS PNS
$Na_{V1.7}$	NaS hNE-Na PN1	SCN9A	Mouse 2 Human 2q24	PNS Schwann cells
$Na_{V1.8}$	SNS PN3 NaNG	SCN10A	Mouse 9 Human 3p22-24	Dorsal Root Ganglion
$Na_{V1.9}$	NaN SNS2 PN5 NaT SCN12A	SCN11A	Mouse 9 Human 3p21-24	PNS

Table 1-1: Mammalian Na_V channels. This table shows the nine members of the voltage-gated Na^+ channels identified, the former names, gene symbol, chromosome location, and the tissues where they are expressed. This nomenclature system was proposed by Goldin et. al. based on the nomenclature of voltage-gated K^+ channels.[23]

FIGURE 1-2

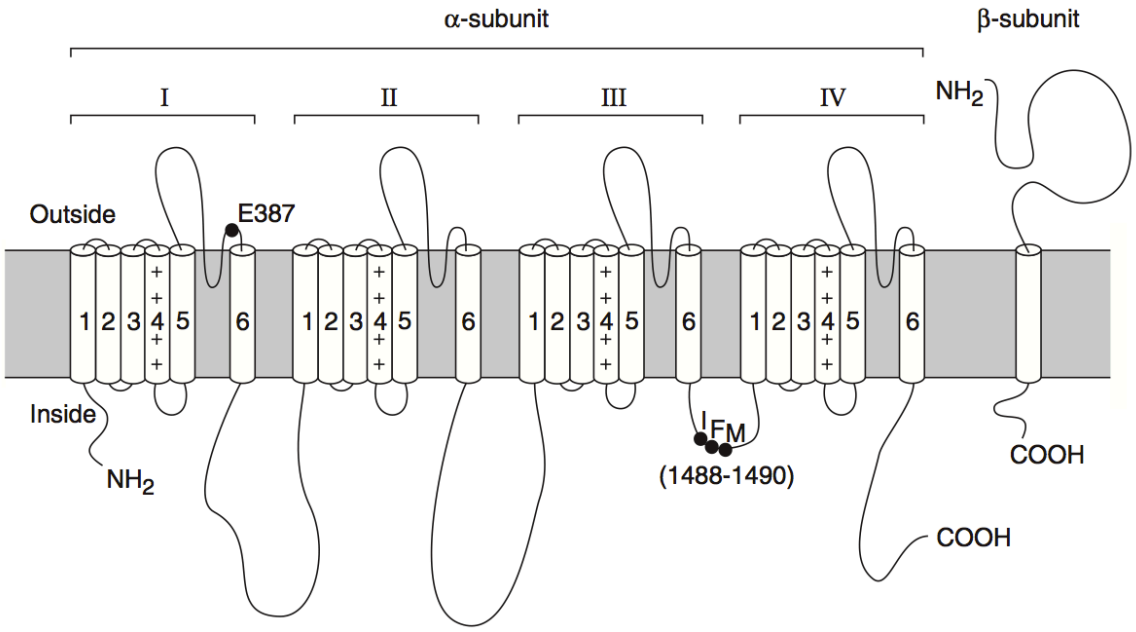

Figure 1-2: Topology of voltage-gated Na^+ channel. Voltage-gated Na^+ channels consist of the α-subunit and the β-subunit. The α-subunit consists of four domains with six segments each. Sequence IFM (1488-1490) in intracellular loop between S6 of domain III and S1 of domain IV is involved in the inactivation process of the Na^+ channel. *(Figure taken from Ashcroft, 2000)*[8]

FIGURE 1-3

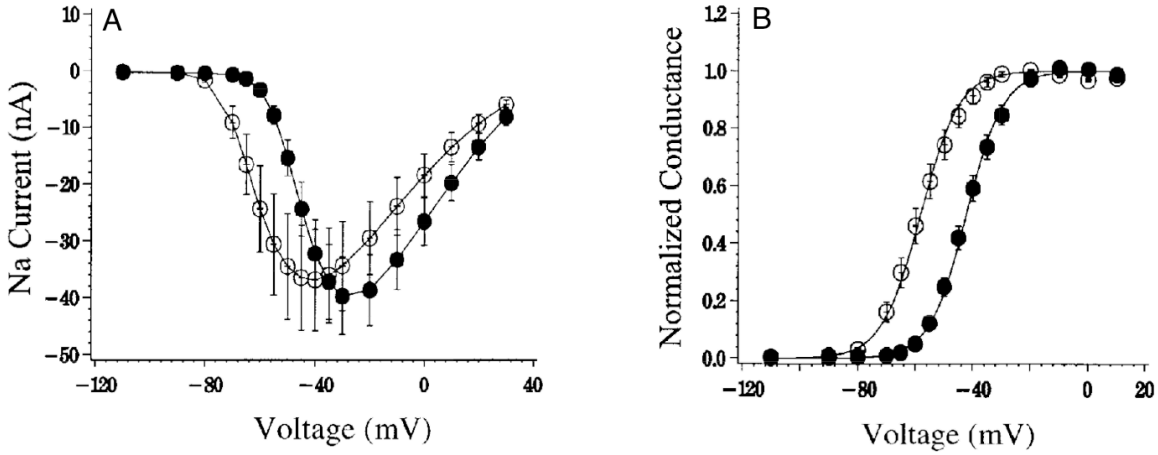

Figure 1-3: Rat skeletal muscle sodium channel (rSkM1) (•) and human cardiac sodium channel (hH1a)(O) I_{Na} expressed in HEK 293 cells. This figure shows a family of I_{Na} responses to step depolarizations between −70 and +30 mV. A) The mean peak I-V relationships for 6 fused cells transfected with rSkM1 and for 5 cells transfected with hH1a. B) The peak conductance-Voltage (G-V) relationships for the same cells as in A with values for each cell normalized to the G_{max} value of each cell. *(Figure and legend adapted from Sheets, 1999)*[30]

Structure-function relationships

The electrophysiological characteristics of Na_V channels (activation, fast inactivation, and slow inactivation) stem from their structures and the way these structures interact with each other.

S4 segments were the obvious candidates for voltage sensing and activation of Na^+ channels due to their unique positively charged residues. The mechanism by which S4 segments act as voltage sensors is not completely understood. However, evidence suggests that the activation process is associated with gating currents (currents that reflect the movement of charges within the membrane). Catterall's sliding helix model provided the best fitting mechanism by which S4 segments allow the passage of Na^+ current in response to depolarization of the membrane. The positively charged residues on S4 segments are stabilized by pairing with negatively charged residues on neighboring segments, locking the helix in a "closed" state. E_m depolarization causes the helix to move outward and rendering the channel "open" (activation).[26, 36] Many site-directed mutagenesis studies provided evidence that S4 segments represent the voltage sensors for Na_V channels. In one of these studies, Stühmer et al[25] replaced one or more positively charged amino acids residues with neutral or negatively charged residues such as glutamine. The more positive charges replaced, the greater the shift towards more positive potentials.

There are also intracellular and extracellular hairpin loops that play important roles in the selectivity and properties of the channel.[16] An important intracellular loop is the one between domains III and IV, which was found to be crucial for fast inactivation. Site-directed antibodies studies were used to narrow down the region of fast inactivation in Na^+ channels to the loop between domains III and IV. In one of these studies, antibodies against

amino acid sequences in intracellular loops between the four domains of the α-subunit were prepared. All the antibodies had no effect on inactivation, except for the antibody directed at the loop between domains III and IV, which slowed fast inactivation. [37] Mutagenesis studies later pinpointed the exact amino acids that are crucial for fast inactivation in Na^+ channels, which were isoleucine (I), phenylalanine (F), and methionine (M) at positions 1488, 1489 and 1490, respectively, are and are often referred to as the IFM cluster (Fig. 1-2). They found that replacing either I or M amino acids by glutamine (Q) significantly slowed inactivation and shifted the fast inactivation curve towards more positive potentials. However, when only F amino acid was replaced by Q, or when all three amino acids IFM were altered to QQQ, fast inactivation was completely abolished. This suggested that F was the most critical of the three amino acids. [38, 39]

Structures involved in activation, fast and slow inactivations are different but related in their interactions. Depolarization leads to movement of S4 and activation. When S4 segments from domain III and IV move, they expose the IFM inactivation cluster and promote fast inactivation. However, when depolarization is prolonged, S4 segments undergo a slower secondary movement, secondary to that of activation. This movement reduces IFM affinity to its binding site, removing fast inactivation, and at the same time occludes the channel rendering it slow-inactivated.[34, 40]

Specific regions involved in slow inactivation are not fully determined, however, it was shown that they are different from fast inactivation. Mutating the IFM cluster removed fast inactivation but slow inactivation remained intact.[38] In addition, different mutations of $Na_{V1.4}$ channels affect different electrophysiological characteristics, giving rise to different channelopathies. For example, G1299E and T1306M mutations in rats, which give rise to

PAM and PMC channelopathies, respectively, cause a defect in the fast inactivation but not the slow inactivation process. On the Other hand, HyperKPP mutations T698M, M1585V and M1353V[†] affect slow inactivation but not fast inactivation (Fig. 1-4 and 1-5).

FROM MUTATION TO HyperKPP

Nine mutations in the SCN4A gene have been identified for HyperKPP.[(6)] The two most common mutations reported are the M1592V (33% of HyperKPP cases), and the T704M (33%), while the remaining 34% of cases correspond to the seven other mutations (Fig. 1-6)

The T704M mutation is located on S5 segment of domain II (Fig. 1-6). Patients with this mutation usually suffer their first paralytic attack within the first year in life. This mutation is also characterized by its more frequent attacks (~16-40 attacks/month) compared to other HyperKPP mutations, but the durations of attacks are shorter (8 ± 28 hours). In comparison, M1592V mutation is located on S6 segment of domain IV (Fig. 1-6), and is characterized by lower frequency of attacks (~1-5 attacks/month), but longer durations compared to other HyperKPP mutations (89 ± 58 hours). Patients with M1592V mutation have their onset of the disease between 1-9 years of age on average, relatively late in childhood compared to patients with T704M mutation. Table 1-2 summarizes the key differences between the two main mutations.[(5, 6)]

[†] M1585V is the homologous rat mutant corresponding to the human M1592V mutation, T697M corresponds to the human T704M mutation, and M1353V corresponds to the human M1360V mutation.[(7)]

FIGURE 1-4

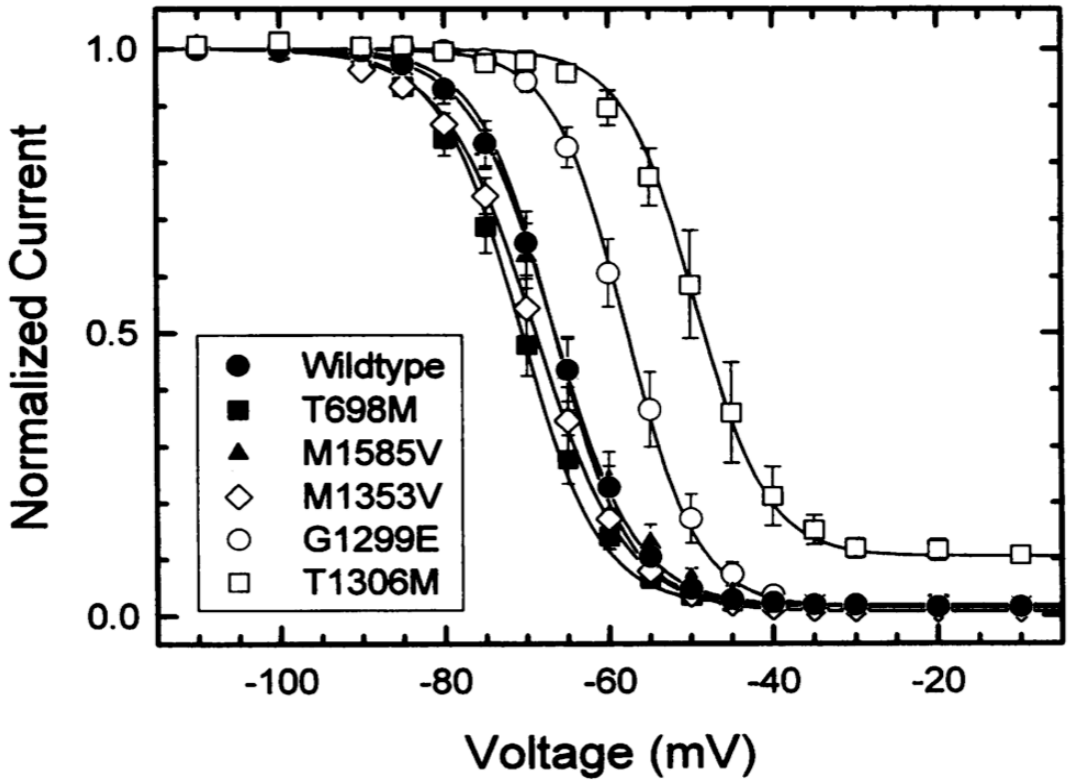

Figure 1-4: Steady-state fast inactivation was not affected in HyperKPP mutations. HyperKPP mutants M1585V, T698M and M1353V (corresponding to the human T704M, M1592V, and M1360V, respectively) did not differ from W.T. measurements and had intact fast inactivation kinetics. Channel availability was measured as the peak Na^+ current was elicited by depolarization to −10 mV, after a conditioning pulse at potentials of −140 to −10 mV (a conditioning pulse is holding the membrane potential at specific voltage for a period of time to measure peak current). Amplitude was normalized to the current after a conditioning pulse at −140 mV. The voltage dependence of steady-state fast inactivation was measured using a fixed 300-ms conditioning pulse. Symbols depict the means ± SEM. *(Figure and legend adapted from Hayward, 1997)*[33]

FIGURE 1-5

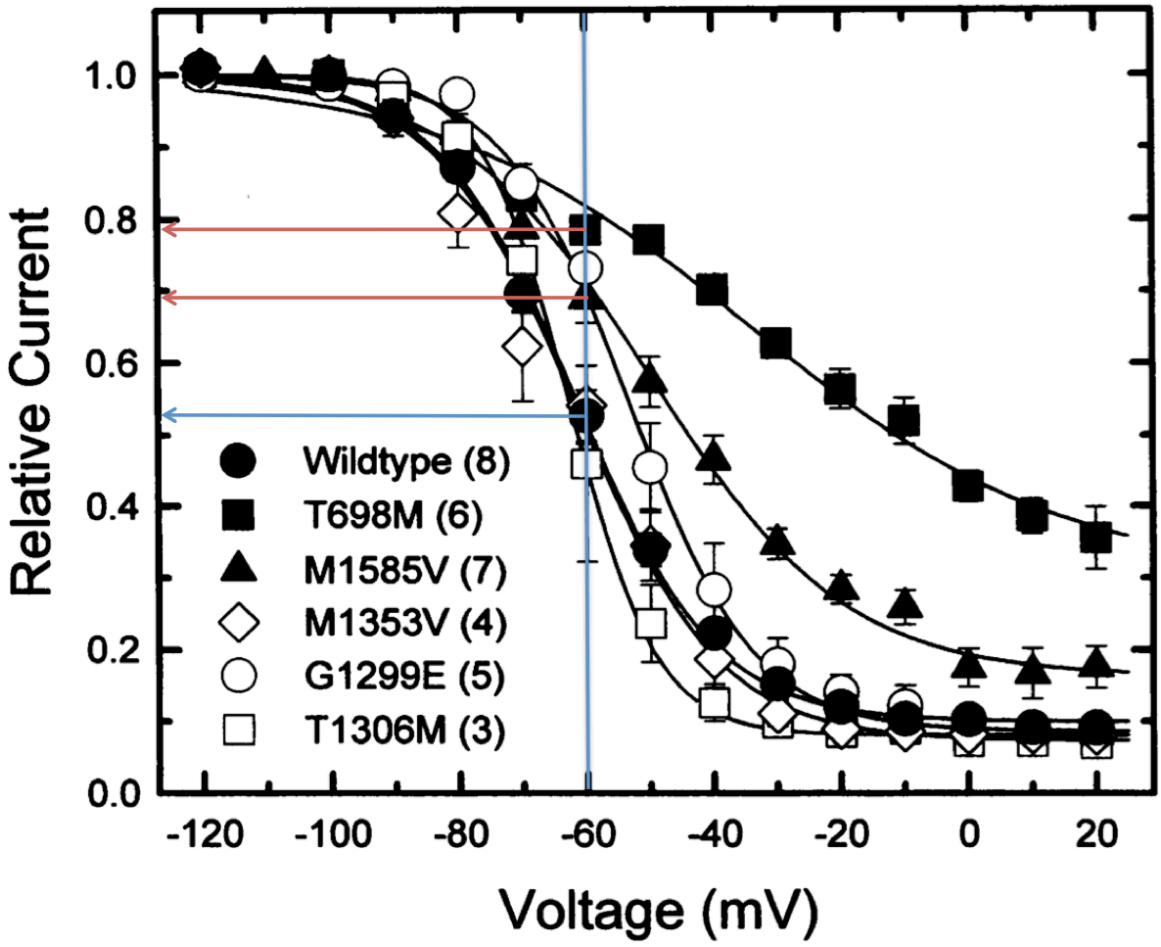

Figure 1-5: Steady-state slow inactivation is defective in HyperKPP's most common mutations. HyperKPP mutations T698M and M1585 (corresponding to the human T704M and M1592V, respectively) show an incomplete slow inactivation *in vitro*. Peak I_{Na}, measured after a 60-s conditioning pulse, was normalized by the peak current elicited from a holding potential of −100 mV. Test and control currents were measured at −10 mV. The conditioning and test pulses were separated by a 20-ms hyperpolarization to −100 mV to allow channels to recover from fast inactivation. *(Figure and legend adapted from Hayward et al, 1997)*[33]

Electrophysiological studies have shown that the two main HyperKPP mutations M1592V and T704M impair the activation processes in $Na_{V1.4}$ channels. Under steady-state conditions, it was shown that the activation curve was shifted by 5-15 mV towards more negative potentials in HyperKPP compared to W.T. channels. This shift enlarged the overlap between steady-state activation and inactivation curves, creating a large Na^+ current window between −75 and −35 mV.[41, 42] In other studies, Hayward et al[33] showed that under steady-sate conditions, fast inactivation was intact in both T704M and M1592V mutations using whole-cell currents from HEK cells (Fig. 1-4). Instead, they reported a defect in the slow inactivation process in mutants characterized by a shift of the slow inactivation curve towards more depolarized membrane potentials (Fig. 1-5). They also showed that, under steady-state conditions and at −60 mV, around 47% of W.T. channels were slow-inactivated, while only 30% of M1585V channels and 20% of T698M channels, were slow-inactivated (Fig. 1-5). Additionally, the rate of entering slow inactivation was significantly slower in both mutations, while the recovery from slow inactivation was faster compared to W.T. channels.[1]

In addition to the defect in $Na_{V1.4}$ channel electrophysiological characteristics, studies have shown that an increase in $[K^+]_e$, has a direct effect on defective $Na_{V1.4}$ channels. Cannon et al[43] using single $Na_{V1.4}$ channel recordings, observed Na^+ currents that inactivated after 4 ms of depolarization in both normal and HyperKPP channels when $[K^+]_e$ was 3.5 mM. However, when $[K^+]_e$ was increased to 10 mM, HyperKPP channels entered a non-inactivating mode with repetitive openings and persistent Na^+ currents past 4 ms of depolarization, which was not observed in normal channels. The K^+-induced non-inactivating Na^+ currents result in a further depolarization of the membrane.

Physiological response to HyperKPP mutations

It has been shown that the incomplete slow inactivation[44] and the defect in activation[41] of $Na_{V1.4}$ channels result in an even larger overlap between the activation and inactivation curves for HyperKPP channels, giving rise to a larger Na^+ current window between −50 and −30 mV.[41, 42] This was manifested as a persistent Na^+ influx in HyperKPP muscles at rest (Fig. 1-7).

A recent study by Clausen et al[45] showed that Na^{22} uptake was 67% higher in Mouse$^{(+/M1592V)}$ than W.T. muscles. It was also shown that the membrane potential of HyperKPP muscles was depolarized by 16 mV compared to W.T. muscles under normal conditions (−73 mV for W.T. vs. −57 mV for mutant muscles). Such depolarizations in HyperKPP muscles are close to the AP threshold of −60 mV. As a result, HyperKPP muscles become susceptible to generating a train of uncontrolled action potentials, known as myotonic discharges that are observed in HyperKPP patients (Fig. 1-7).

Myotonic discharges then lead to an increase in t-tubular, interstitial, and plasma K^+. This causes further depolarization because of the K^+-induced non-inactivating Na^+ current, making HyperKPP patients even more sensitive to elevations in $[K^+]_e$. In a series of clinical studies conducted to test the effect of increased $[K^+]_e$ on membrane potential in HyperKPP muscles, it was shown that increasing $[K^+]_e$ from 3.5 mM to 10 mM depolarized the membrane to −55 mV in HyperKPP fibers compared to −61 mV in normal fibers. In addition, when $[K^+]_e$ was lowered back to 3.5 mM, normal fibers repolarized rapidly to normal resting potentials while HyperKPP fibers had a slower repolarization rate.[21, 44]

In addition to its depolarizing effect, increased $[K^+]_e$ was also linked to force depression. The depressive effects of K^+ on force have been shown in many studies

involving healthy subjects.[46] However, electrophysiological studies have shown that HyperKPP patients are more sensitive to elevation in $[K^+]_e$ than healthy individuals and that this sensitivity is related to the K^+-induced depolarization effect. Lehmann-Horn et al[44] showed that increasing $[K^+]_e$ to 10 mM completely abolished twitch force in HyperKPP patients compared to mild force depression in normal subjects. Furthermore, Hayward et al[7] tested the effect of elevated $[K^+]_e$ on tetanic force of W.T. and HyperKPP extensor digitorum longus muscles (EDL) at 25°C. Increasing $[K^+]_e$ from 4 mM to 8 mM did not have an effect on W.T. muscles, however, it induced a 40% decrease in tetanic force in HyperKPP muscles. In addition, when $[K^+]_e$ was further increased to 10 mM, tetanic force in W.T. muscles decreased only by 20% compared to a 90% decrease in force in HyperKPP muscles.

Therefore, it was proposed that when the K^+-induced depolarization is large enough in HyperKPP heterozygotes, it could inactivate all normal $Na_{V1.4}$ and some defective $Na_{V1.4}$ channels. As a result, not enough $Na_{V1.4}$ channels are available to generate APs rendering the muscle fiber inexcitable, and consequently paralysis occurs. Therefore, myotonic discharges are usually followed by a complete paralysis (Fig. 1-7).

Other physiological responses in HyperKPP

In addition to the myotonic discharges and paralysis observed in HyperKPP patients and Mouse$^{(+/M1592V)}$, studies have also shown a shift towards myosin IIA and oxidative fiber types in HyperKPP muscles.[4, 7] Mammalian skeletal muscles are a mixture of different fiber types that are classified mainly according to the myosin heavy chain isoform (MHC). Four MHC isoforms are expressed in the adult muscle fiber: MHC-I, MHC-IIA, MHC-IIX and

MHC-IIB. In general, MHC-I fibers have the slowest contractions and a high oxidative capacity. On the other extreme, MHC-IIB fibers have fastest contractions and a high glycolytic capacity.[47] The other two types of fibers, MHC-IIA and MHC-IIX, are both fast fibers, however, MHC-IIA fibers are oxidative, whereas MHC-IIX fibers are glycolytic. [47-50] In addition to the unique expression of each fiber type, there are hybrid fibers that express two or more MHC isoforms.[51]

Early studies in the 1940s showed that fiber types were flexible and could transform from one isoform to another depending on nerve stimulation patterns.[52] Generally, fiber types can shift towards oxidative fibers as a result of slow *in vitro* stimulation, aerobic exercise and endurance training as well as hypothyroidism. By contrast, fibers can have a shift towards glycolytic fibers by fast *in vitro* stimulation, denervation, resistance training and hyperthyroidism. In HyperKPP, shifts towards oxidative fibers were observed.[7] It was proposed that the myotonic discharges in HyperKPP resemble *in vitro* chronic low frequency stimulation (CLFS) since both induce shift towards oxidative fibers.[7, 53-56] In addition, endurance training also promotes fiber type transitions towards oxidative fibers, suggesting a common pathway.[57] Therefore, the following review focuses on the effect of slow *in vitro* stimulation and endurance exercise on fiber type transition.

FIGURE 1-6

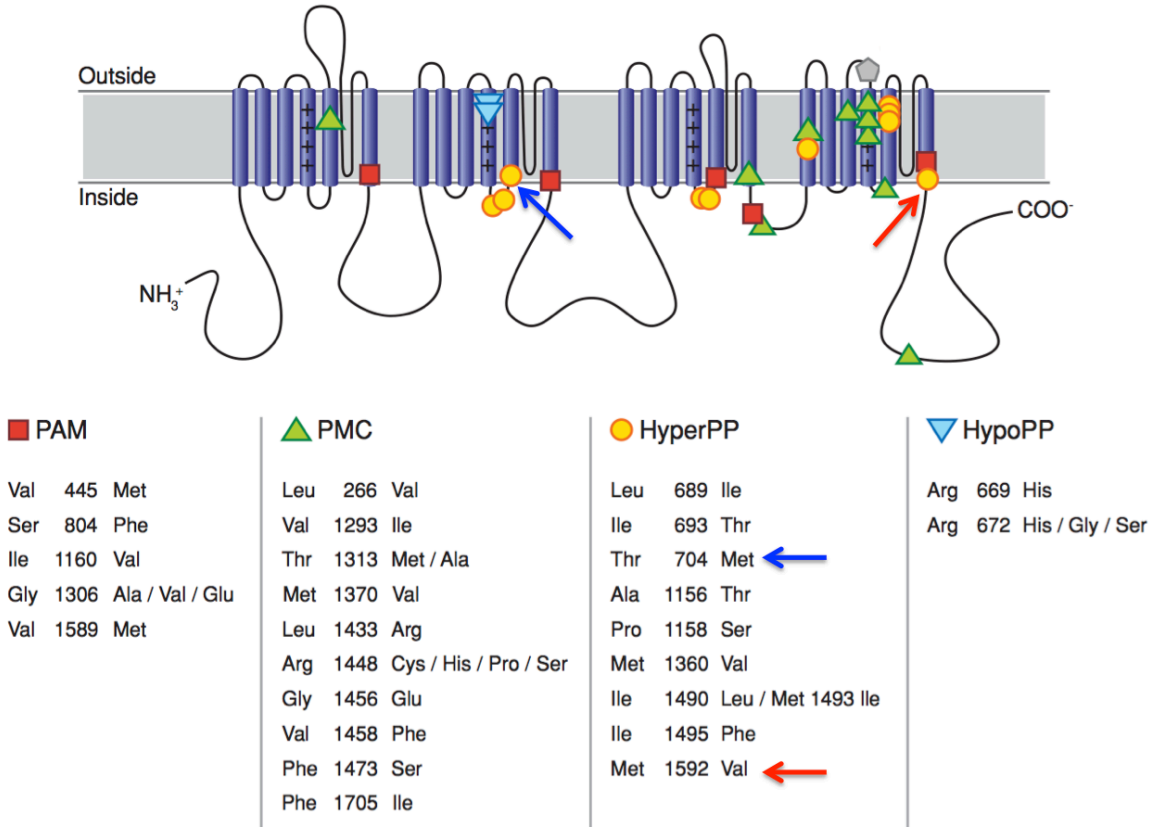

Figure 1-6: Missense mutations in $Na_{V1.4}$ associated with HyperKPP and other channelopathies. The diagram of the α-subunit of $Na_{V1.4}$ channel shows the relative locations of missense mutations associated with PAM, PMC, HyperKPP, and HypoKPP. The two most common mutations of HyperKPP are: T704M located on S5 segment of domain II (*blue arrows*), and M1592V located on S6 segment of domain IV (*red arrows*). *(Figure adapted from Cannon, 2006)*[15]

TABLE 1-2

Summary findings	T704M mutation (n = 50)	M1592V (n = 13)	All HyperKPP mutations (n = 82)
Age at onset, y	0.8 ± 0.8	5 ± 4	2 ± 4
Average ± SD	0–0.9	0–10	0–16
	(n = 39)	(n = 13)	(n = 63)
Frequency of attacks/mo			
Average ± SD	28 ± 12	3 ± 2	16 ± −16
Range	8–42	5–6	1–42
	(n = 17)	(n = 4)	(n = 26)
Duration, h			
Average ± SD	8 ± 28	89 ± 58	24 ± 42
Range	0.3–168	24–144	2–72
	(n = 41)	(n = 7)	(n = 56)
Usual precipitants, %			
Exercise	83	73	80
Cold	58	38	54
Hunger	29	13	25
Stress	46	13	34
Illness	0	38	30
Potassium rich foods	32		21
Other	25	38	8
	(n = 41)	(n = 11)	(n = 64)

Table 1-2: Clinical data for HyperKPP. Eighty-two patients with HyperKPP mutations were examined, 50 of them had T704M mutation, 13 had M1592V mutation, while the other 19 had one of the other HyperKPP mutations. The key differences between the two most common mutations are in the age of onset, the frequency, and duration of attacks (*red boxes*). *(Table adapted from Miller et al, 2004)*[5]

FIGURE 1-7

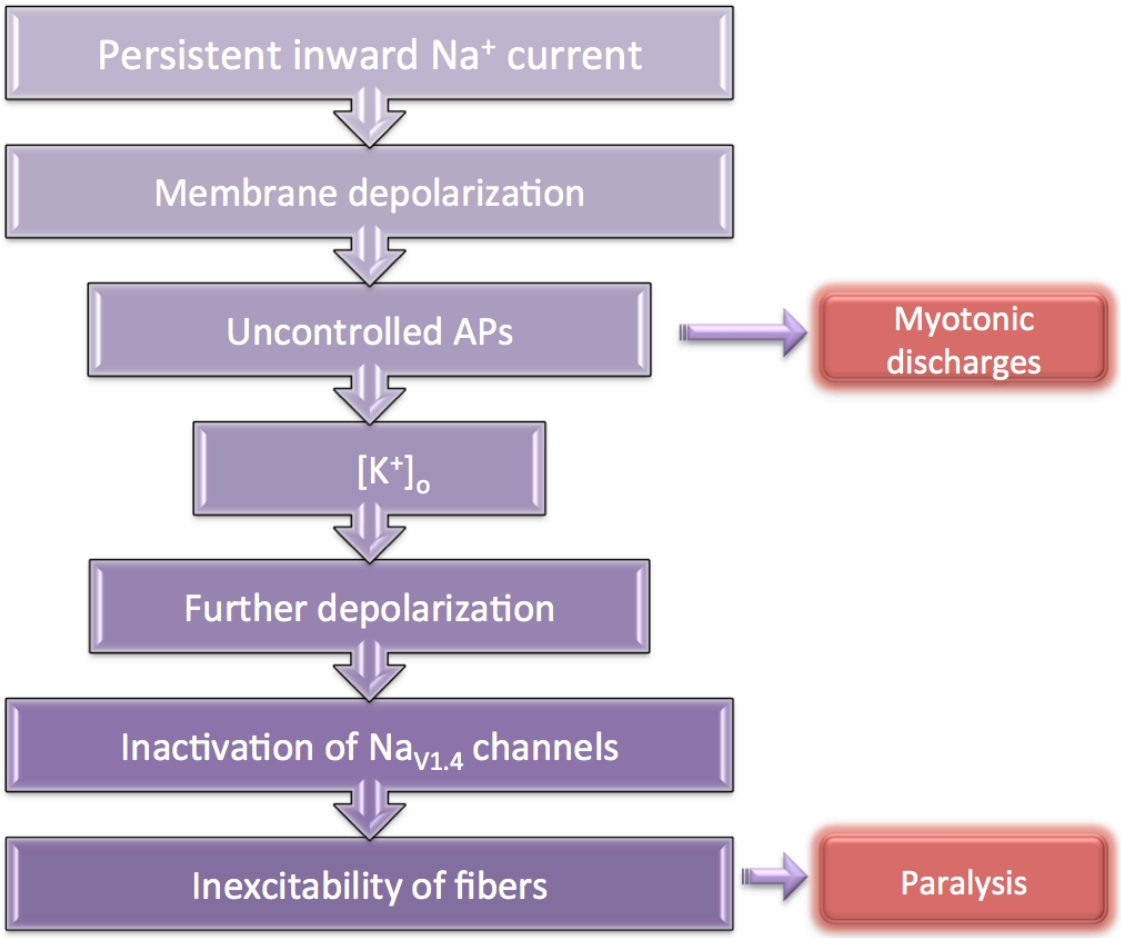

Figure 1-7: A schematic diagram showing the physiological response to the defect in $Na_{V1.4}$ channels. HyperKPP most common mutations in $Na_{V1.4}$ channel cause an incomplete inactivation of these channels. This leads to a persistent Na^+ current that keeps the membrane at depolarized potentials and close to AP threshold. Myotonic discharges arise when AP threshold is reached leading to a train of uncontrolled APs which in turn increases $[K^+]_e$. A large increase in $[K^+]_e$ cause further depolarization of the membrane, which can lead to the inactivation of Na^+ channels causing inexcitability of the membrane and paralysis.

Changes in fiber type composition are complex processes. Endurance exercise, as well as and CLFS and HyperKPP myotonic discharges, increase $[Ca^{2+}]_i$, which was shown to activate calcineurin, a Ca^{2+}-regulated phosphatase.[58, 59] Activated calcineurin in turn causes the translocation of nuclear factor of activated T cells (NFAT) from the cytosol to the nucleus. As a result of this translocation, NFAT is able to bind to DNA and along with other transcriptional regulators, such as myocyte enhancer factor 2 (MEF2), to promote the expression of oxidative fiber types.[59, 60]

Another key player in the oxidative pathway is peroxisome-proliferator-activated receptor-gamma coactivator-1 or PPARγ1 (PGC-1α). Studies have shown that over-expression of PGC-1α in transgenic mice increased the expression of oxidative fiber types, as well as mitochondrial biogenesis, angiogenesis and oxidative metabolism.[61, 62] The exact pathway by which PGC-1α gets activated is not well understood, but many studies showed that it could be activated as a result of endurance exercise and CLFS.[61, 63] This is also true for HyperKPP muscles, where PGC-1α levels were found to be elevated in the TA muscles of HyperKPP compared to W.T. mice.[7]

In summary, HyperKPP is a complex and an unpredictable disease. Current treatments are not fully effective and overtime they lose their effect. Their mechanism of action is also not understood.[21, 22] While the symptoms of myotonic discharges and paralysis could be explained in relation to the defect in $Na_{V1.4}$ channels, it is not understood why there is an asymptomatic period and a worsening of symptoms with age. In order to develop better pharmacological treatments, one must better understand the disease. Therefore, and as a first step, this project tries to determine the reason for the asymptomatic period despite expressing $Na_{V1.4}$ channels, by proposing one of two mechanisms.

The first mechanism suggests that all symptoms are due the defective $Na_{V1.4}$ channel content and/or activity (Na^+ influx). In this case, $Na_{V1.4}$ content and/or activity may reach a critical threshold, after which the onset of symptoms occurs. The rationale behind this mechanism was based on developmental studies that showed an increase in $Na_{V1.4}$ channel content and activity with age. In one study, $Na_{V1.4}$ mRNA content during the first five years of life in humans was shown to be between 20%-30% of the adult content. The expression then increased dramatically after five years of age until adulthood (Fig. 1-8A). The exact age at which $Na_{V1.4}$ channel content reach a maximum in humans was not known, but the increase between 5 years of age and adulthood could be the reason behind the increase in symptoms with age. In mice and during prenatal development, mRNA of both $Na_{V1.5}$ channels (embryonic isoform) and $Na_{V1.4}$ are expressed in skeletal muscles. Postnatally, however, $Na_{V1.5}$ content starts to diminish and $Na_{V1.4}$ content increases reaching a maximum content by 3-4 weeks of age (Fig. 1-8B).[17] Another study showed that I_{Na} density in rats increased from 10 mA/cm^2 at 0-5 days of age to about 85 mA/cm^2 in adult muscles, which were at least 3 months old. [64]

$Na_{V1.4}$ channel content in humans does not change between infancy and 5 years of age (Fig. 1-8A). However, the onset of paralysis occurs during the first year of age in patients with T704M mutation and may occur before 5 years of age in patients with M1592V mutation. This suggest the involvement of factors other than $Na_{V1.4}$ channel content or activity. Therefore, the other mechanism suggests that some symptoms (myotonic discharges) may start with the defective $Na_{V1.4}$ channels; while other symptoms (paralysis) occur after changes in other membrane components occur. Such changes include modifying gene expression, which may alter the expression and/or activity of other ion channels and

ultimately changing membrane conductance. The fiber type shift observed in HyperKPP muscles support that changes in gene expression do occur in HyperKPP.

Another interesting feature of HyperKPP is the sparing of the diaphragm muscle from symptoms despite expressing defective $Na_{V1.4}$ channels.[5] This indicates that the diaphragm, unlike other muscles, may have a special mechanism that protects it against paralysis. *In vitro* studies carried out for this project showed that the diaphragm did not present contractile defects confirming the sparing of the diaphragm in Mouse$^{(+/M1592V)}$ (Barbalinardo and Renaud, unpublished results). In addition, flexor digitorum brevis muscles (FDB) also showed minimum contractile defects, while EDL and soleus muscles showed significant contractile defects *in vitro* (Dejong and Renaud).

FIGURE 1-8

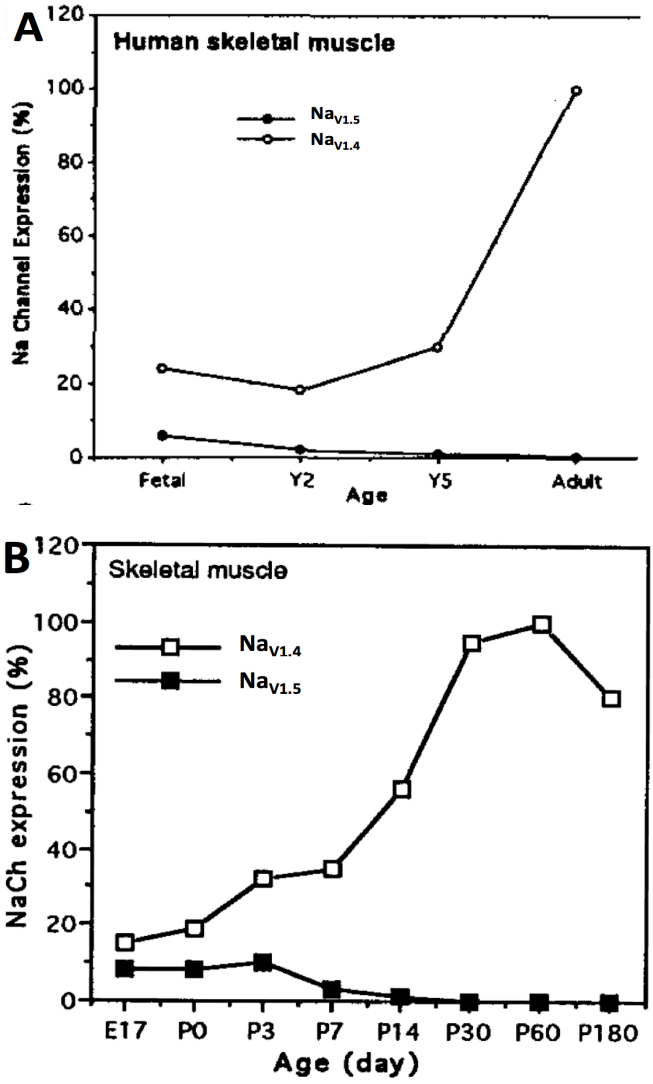

Figure 1-8: Sodium channels mRNA expression in human skeletal muscle (A) and in mouse skeletal muscle (B). The adult $Na_{V1.4}$ channel mRNA increases while the embryonic $Na_{V1.5}$ channel mRNA decreases with age. For each age, Quantitative Multiplex Fluorescence PCR (QMF-PCR) was performed for actin fetal Na^+ channel, and adult Na^+ channel mRNAs. The values were normalized to adult Na^+ channel mRNA expression in adult skeletal muscle. E17= embryonic day 17. P0= neonate. P3= postnatal day 3. Y2= 2 years of age. *(Figures and legend adapted from Zhou & Hoffman, 1994)*[17]

OBJECTIVES AND HYPOTHESES

For this project, a series of studies were undertaken in an attempt to untangle the complexity of HyperKPP and answer the questions mentioned previously. *In vitro* and *in vivo* studies were carried out to follow the progression of HyperKPP with age in relation to changes in $Na_{V1.4}$ content and activity. The objective of this specific study was to follow these changes *in vivo*. Considering the aforementioned possibilities, the main objectives of this study were to examine when the onset of the paralysis occurred in relation to $Na_{V1.4}$ content and activity, to quantify changes in fiber types in various muscles including the diaphragm, and to follow the progression of fiber damage with age.

Hypothesis 1: The defect in $Na_{V1.4}$ channels is the only factor responsible for the onset and progression of symptoms.

Hypothesis 2: If the diaphragm and FDB muscles in Mouse$^{(+/M1592V)}$ are spared from HyperKPP symptoms, then changes in fiber type would not occur.

To test these hypotheses using Mouse$^{(+/M1592V)}$, the specific aims of this study were:

(1) To determine the onset of paralysis and monitor its progression with age, using rest after exercise as a trigger;

(2) To follow the exercise capacity of HyperKPP mice with age;

(3) To examine changes in fiber types in EDL, soleus, diaphragm and FDB muscles, and determine whether these changes, if any, coincide with or follow the onset of paralysis;

(4) To verify that the diaphragm and FDB muscles in HyperKPP do not show changes in fiber type composition, and that EDL and soleus muscles show the most changes in fiber type composition; and

(5) To follow fiber damage in HyperKPP muscles with age.

CHAPTER 2

MATERIALS AND METHODS

MATERIALS

Chemicals and materials employed in this study are summarized in Appendix 1.

METHODS

MOUSE MODEL

The experimental mouse model used in this project was generated by Dr. Hayward and colleagues in 2008. The mouse was generated by knocking in a missense substitution corresponding to the human M1592V mutation in the mouse gene encoding the $Na_{V1.4}$ channel (SCN4A). This Met-to-Val mutation is located at position 1586 of the mouse $NaV_{1.4}$ α-subunit, which is the equivalent of the 1592 position in humans.[7] Heterozygous mice exhibited similar HyperKPP features to human patients such as myotonic activity *in vivo*, greater reduction of force at increased $[K^+]_e$ *in vitro* in HyperKPP than in W.T. mice, alleviation of weakness with increased $[Ca^{2+}]_i$ *in vitro*, an increase in oxidative capacity of glycolytic muscles, as well as muscle damage and observation of central nuclei. Most homozygous mice die during their first month of life; therefore, only heterozygous mice were used in this study. Furthermore, the experimental mice were generated using the FVB mice strain; therefore, FVB mice were used as the wild type control.

Mice used in this study were 2 weeks to 12 months of age. They were fed *ad libitum* and housed according to the guidelines of the Canadian Council for Animal Care. All

experimental procedures in this study were approved by The Animal Care Committee of the University of Ottawa. Before the mice were sacrificed, they were anaesthetized with a single 0.05-0.07ml shot of 2.2mg Ketamine/0.4 mg xylazine/0.22 mg acepromazine cocktail.

The Age groups used for this study were: 2 weeks, 3 weeks, 1, 2, 3, 4, 6, 9, and 12 months old. Each age group consisted of a rest group and an exercised group of both W.T. and HyperKPP mice. Due to difficulties eliciting 2-week-old mice to run, only the rest group was studied for this age.

GENOTYPING

Day1

DNA Extraction. All animals used in this study were genotyped using a ~0.5 mm segment of the tail. Segments were placed in 1.5 ml Eppendorf tubes and lysed by overnight incubation with 600 µl tail digestion buffer (1 M Tris-pH 8.0, 5 M NaCl, 0.5 M EDTA-pH 8.0, 10% SDS) and 50 µl Proteinase-K (10 mg/ml) at 56°C. A negative control (no tail) was used to test for any contamination.

Day 2:

A volume of 650 µl of 1:1 phenol:CIA was added to each tube, mixed thoroughly, then centrifuged at 12,000 g for 10 min. The top aqueous layer was carefully transferred to another tube, extracted again with 650 µl CIA to remove the phenol, vortexed, and centrifuged for 10 min. Strands of DNA were precipitated by mixing the top aqueous layer with 750 µl of isopropyl alcohol at RT. After 10 min, tubes were centrifuged for 10 min and DNA pellets formed at the bottom of the tubes. Excess supernatant was removed, 750 µl of 70% ethanol was added to wash away salts, and centrifuged again for 10 min. Supernatants

were removed, pellets were air dried for 30 min, re-suspended in 200 µl of 1x TE buffer (10 mM Tris, 1 mM EDTA-pH 8.0) and incubated at 66°C for 2 hours. DNA samples were then stored at 4°C until ready for PRC procedure.

PCR and restriction digest. A PCR sample contained 1 µl of DNA sample and 49 µl of master mix (25 µl 2x Phusion buffer, 20.5 µl DNAse-free H_2O, 1.5 µl DMSO, 1 µl NC1F forward primer, and 1 µl FC2R reverse primer). The template primers were mSk757F, 5'TACTACTTCACCATTGGCTGGATATCTTCGACTTCG-3' at the 3' end of exon 23, and mSk998R, 5'CTGAGCACAATCTCCATTTCCCTCAGC-3' in the 3'-UTR of exon 24. The PCR protocol had the following cycles: 80°C - 10 seconds / 99°C- 1 minute / 45 cycles of: 98°C - 10 seconds / 67°C - 30 seconds / 72°C - 30 seconds / End of 45 cycles: 72°C - 7 minutes.

For digestion, 10 µl of PCR product was added to 10 µl of digestion enzyme NSP1 mixture (7.3 µl DNAse-free H_2O, 2 µl buffer 2, 0.5 µl NSP1, and 0.2 µl BSA). The samples were incubated overnight at 37°C.

Day 3:

Gel electrophoresis. A gel was prepared using 2.25 g agarose, 150 ml TBE buffer, and 5.5 µl Ethidium Bromide. When the gel was ready, 10 µl of restriction digest product was loaded into wells along with a 100 bp DNA ladder. Gel ran at 100V for 45 minutes.

FREQUENCY OF PARALYSIS AND EXERCISE CAPACITY

W.T. and HyperKPP mice were elicited to run on a treadmill. Food was removed from the cages 30-45 minutes before the start of the exercise. Mice were made comfortable with the treadmill by placing them on it for five minutes before the treadmill was turned on. Mice ran simultaneously on individual lanes and weight was taken before and after the

exercise to account for water loss and body weigh influence. No electrical shock was used. Instead, a sponge was placed halfway into the lane to stimulate mice to run forward when they touched it.

The exercise began with a 15°-uphill-angle and a speed of 10 m/min. Every five minutes, speed was increased to 15 m/min, 20 m/min, and 25 m/min and left at 25 m/min for a maximum of 45 minutes. Mice were withdrawn from the treadmill once they no longer maintained the required pace. This occurred when a mouse was mostly leaning on the sponge and did not continue running despite stimulating the tail with a pencil for 10 consecutive seconds. Mice were exercised using this protocol once a day for five consecutive days at various times of the day.

After the fifth day of exercise, distances run by each mouse were calculated as the product of speed and time spent by each mouse at each speed. For example, a mouse that spent 20 minutes on the treadmill meant that it ran five minutes at each speed. The distance run at each speed was then calculated as 50, 75, 100 and 149.2 m. The sum of these distances would be the total distance run by the mouse that day, 374.2 m.

Age groups used for this protocol were: 3 weeks, 1, 2, 3, 4, 9, and 12 months of age. During the exercise days, HyperKPP mice from all age groups were monitored for presentation of paralysis before, during, or after the exercise. At the end of the exercise week, all exercised animals along with their non-exercised counterparts were sacrificed and muscles were collected.

MUSCLE PREPARATION

EDL, soleus, FDB, and diaphragm muscles were dissected on a dry petri dish to prevent freezing artifacts. Muscles were embedded in a small amount of cooled OCT compound and frozen in isopentane pre-cooled in liquid nitrogen. Muscles were stored at -80°C until used.

For histology, 10 μm cross sections were cut at the mid-belly of the muscle using a cryostat (Leica Microtome, HM 500M) cooled to -19°C, mounted on positively charged slides (Superfrost/Plus, Fisher Scientific, USA), and stored at -80°C until used.

MYOSIN FIBER TYPES

Immuno-histochemical analysis was used to determine the fiber type composition of muscles. Serial cross sections were double-stained with anti-laminin primary antibody and either anti-MHC I, IIA, IIB or IIX antibodies (Table 2-1). Anti-laminin antibody was used to better identify boundaries between individual fibers.

For myosin MHC-I, MHC-IIA and MHC-IIB staining, slides were placed on a slide dryer (set at 37°C) for 15 minutes and then rinsed in 1X Phosphate Buffered Saline (PBS) (pH 7.2-7.4) for 3 minutes. Sections were blocked with 0.5% Bovine Serum Albumin (BSA) in PBS for 1-hr at room temperature in a humid chamber. Sections were exposed to the primary antibodies for two hours at RT in a humid chamber. The antibodies were removed; cross-sections rinsed in PBS 3 times, 5 min each time. Sections were incubated with secondary antibodies (Table 2-1) for 45 minutes at 37°C in a humid chamber, and rinsed 3 times in PBS. Secondary antibodies were diluted in triton-X 100 solution. Sections were mounted with anti-fade reagent, and stored at -80°C until viewed. Control sections were also

stained without the primary antibody to test for non-specific secondary antibody binding.

For MHC-IIX, the staining protocol was slightly modified to enhance primary antibody binding and block non-specific binding (personal communication with Dr. J. von Maltzahn). After sections were thawed on the slide dryer, they were fixed in 100% ethanol for 5 minutes then rinsed in PBS kept at pH of 7.4. Sections were blocked with 5% horse serum (HS) in PBS, and incubated with primary antibodies overnight at 4°C. The next day, sections were rinsed 3 times in PBS for 5 min each time, and incubated with secondary antibodies for 1-hr at RT. Secondary antibodies were diluted in 5% HS blocking solution. Sections were rinsed again in PBS, mounted with anti-fade reagent, and kept at -80°C until viewed.

FIBER DAMAGE

Muscle cross-sections were stained with hematoxylin and eosin (H&E) to detect any morphological changes or damage in W.T. and HyperKPP muscle fibers, i.e. central nuclei or vacuolization.

Sections were dried on a slide dryer (set at 37°C) for 15 min then fixed in 10% formalin for another 15 min. Sections were briefly rinsed in tap water then in distilled water before they were exposed to hematoxylin solution for 7 min. Slides were rinsed until clean in tap water then dipped 4 times in 1% acid alcohol (5 drops of concentrated hydrochloric acid in 250 ml of 70% ethanol). Slides were rinsed with tap water for 5 min then dipped in 0.5% Lithium carbonate (Li_2CO_3) for 1.5 min. Slides were returned to tap water for another 5 min. Slides were immersed in 70% ethanol for 1 minute followed by 10 dips in eosin diluted with 70% ethanol. Slides were dipped in 95% ethanol for 2 min, followed by 2 min in 100% ethanol before being dipped in toluene for 3-4 minutes. Finally, sections were

covered with coverslips using one drop of permount mounting medium and stored at RT until viewed.

IMAGE ACQUISITION AND ANALYSIS

All immunofluorescent images in this study were captured using a Sony digital camera (model DXC-950, Canada) attached to an Axiophot-2 mot *plus* fluorescence microscope (Zeiss, Canada). The image acquisition software used for capturing and analyzing the images was Northern Eclipse (EMPIX Inc., USA). Due to variations in anti-myosin staining between muscles, acquisition settings (exposure time, gain, offset, and binning) were optimized for each muscle in an attempt to minimize background and maximize the visibility of positive fibers for quantitative analysis. Immunofluorescent images were captured using 10x and 20x objectives.

For quantitative analysis of different myosin types, positive fibers with high fluorescence intensity, lower fluorescence intensity, and negative fibers were manually counted using Northern Eclipse software. High and low fluorescence intensity fibers were manually counted as positive fibers and expressed as a percentage of the total number of fibers as presented in the results section.

Images of fibers stained with H&E were captured using the bright field of Ziess Axiophot microscope (Zaiss, Canada). H&E images were captured using 10x and 20x objectives. The total number of fibers with central nuclei was manually counted and expressed as a percentage of the total number of fibers.

STATISTICAL ANALYSIS

Data are presented as means ± S.E. Split plot ANOVA was used to determine

significant differences. ANOVA calculations were made using the version 9.2 GLM (General Linear Model) procedures of the Statistical Analysis Software (SAS Institute Inc., Cary, NC, USA). When a main effect or an interaction was significant, the least square difference (LSD) was used to locate the significant differences.[65] The word "significant" refers only to a statistical difference ($P < 0.05$).

TABLE 2-1

Primary Antibody	Isotype	Dilution	Source
A4.840 Anti MHC-I	Mouse IgM	None	Mouse Hybridoma (DSHB, U Iowa) Cat.# A4.840
SC-71 Anti MHC-IIA	Mouse IgG	None	Mouse Hybridoma (DSHB, U Iowa) Cat.# SC.71
BF-F3 Anti MHC-IIB	Mouse IgM	None	Mouse Hybridoma (DSHB, U Iowa) Cat.# BF-F3
6H1 Anti MHC-IIX	Mouse IgM	None	Mouse Hybridoma (DSHB, U Iowa) Cat.# 6H1
Anti-Laminin	Rabbit IgG	1:1000	Sigma-Aldrich, Canada Cat.# L-9393
Secondary Antibody	**Isotype**	**Dilution**	**Source**
FITC-conjugated Goat-anti-Mouse	Goat IgG	1:200	Sigma-Aldrich, Canada Cat.#F4143
FITC-conjugated Goat-anti-Mouse	Goat IgM	1:200	Chemicon Cat.# AP128F
Rhodamine-conjugated Goat-anti-Rabbit	Goat IgG	1:200	Jackson Laboratories Cat.# 111-025-144

Table 2-1: Antibodies used for immuno-histochemical analysis. All commercially supplied primary and secondary antibodies were diluted with 0.3% Triton-X 100 in 1X PBS solution. The MHC antibodies were used as undiluted supernatants collected from hybridoma cultures.

CHAPTER 3

RESULTS

FREQUENCY OF PARALYSIS AND EXERCISE CAPACITY

In humans, the two most consistent triggers for paralysis are ingestion of K^+ salts (triggers the symptoms 100% of the time) and rest after exercise (80%).[5] In this study, exercise was chosen over K^+ salts ingestion for two reasons: first, high plasma K^+ may cause heart problems in mice; and second, to examine exercise capacity of HyperKPP mice.

Mice were elicited to run on a treadmill daily for five consecutive days and were constantly observed during exercise sessions, which typically lasted 1-2 hours. Contrary to humans for which paralysis was triggered after exercise, in Mouse$^{(+/M1592V)}$, paralysis was randomly observed before, during, and after exercise. Paralysis was visualized with the naked eye in HyperKPP mice. It was characterized by hind limbs being dragged behind the body (Fig. 3-1A and B), or mice lying on their sides (Fig. 3-1C). Typically, the attacks were brief, lasting 10 to 30 seconds.

Paralysis was seen in only one of the six 3-week-old HyperKPP mice (Table 3-1). The largest number of animals observed paralyzed was at 1 month of age, as paralysis was seen in six of the seven HyperKPP mice tested. At 2 months of age, the number of observed paralytic attacks was much less. Paralysis was not observed in 3-6 months old HyperKPP mice, but was observed in few 9 and 12 months old mice.

HyperKPP mice did not necessarily have a paralytic attack every day. For mice observed with paralytic attacks, the average number of days an attack was seen is indicated in Table

3-1. Not only did more HyperKPP mice present paralysis at 1 month of age, but they also exhibited it more frequently than any other age group averaging 3.2 days out of five.

At some ages, the distance run by W.T. mice changed very little over the five days of exercise. For example, W.T. mice at 3 weeks of age only improved their running capacity by 1.3 fold, from 249 m on day one to 329 m on day five (Fig. 3-2A). At other ages such as 2 months, the distance run by W.T. mice increased significantly over the five consecutive days of running (Fig. 3-2B). These mice were able to improve their running capacity from 326 m on day one to 871 m on day five, representing a 2.6-fold-increase.

Just like their W.T. counterparts, HyperKPP mice at 3 weeks of age showed no improvement in their running capacity, but had a tendency to run slightly shorter distances on day 1, 3 and 5 (Fig. 3-2A). Contrary to 2-month-old W.T. mice, 2-months-old HyperKPP mice struggled to improve their running distances from 314 m on day one to 423 m on day five, which represented just a 1.3-fold-increase (Fig. 3-2B).

On the first day of exercise, most W.T. mice between 3 weeks and 12 months of age ran on average between 162 and 327 m, except for 3-month-old mice for which the average distance was 430 m (Fig. 3-3A). Performance improved over the five days of exercise only between the ages of 1 and 4 months (Fig.3-3B). Distances run by W.T. mice between 1-3 months ranged from 818-934 m on day five, compared to 319-430 m on day one. Although mice at 4 months of age also improved their running capacity on day five compared to day one, the improvement observed was less than that of younger mice. At 4 months of age, mice improved by only 298 m compared to the 499-544 m for 1-3 months old mice. W.T. mice at 9 and 12 months of age, did not improve their running capacity from day one to day five (Fig. 3-3B).

FIGURE 3-1

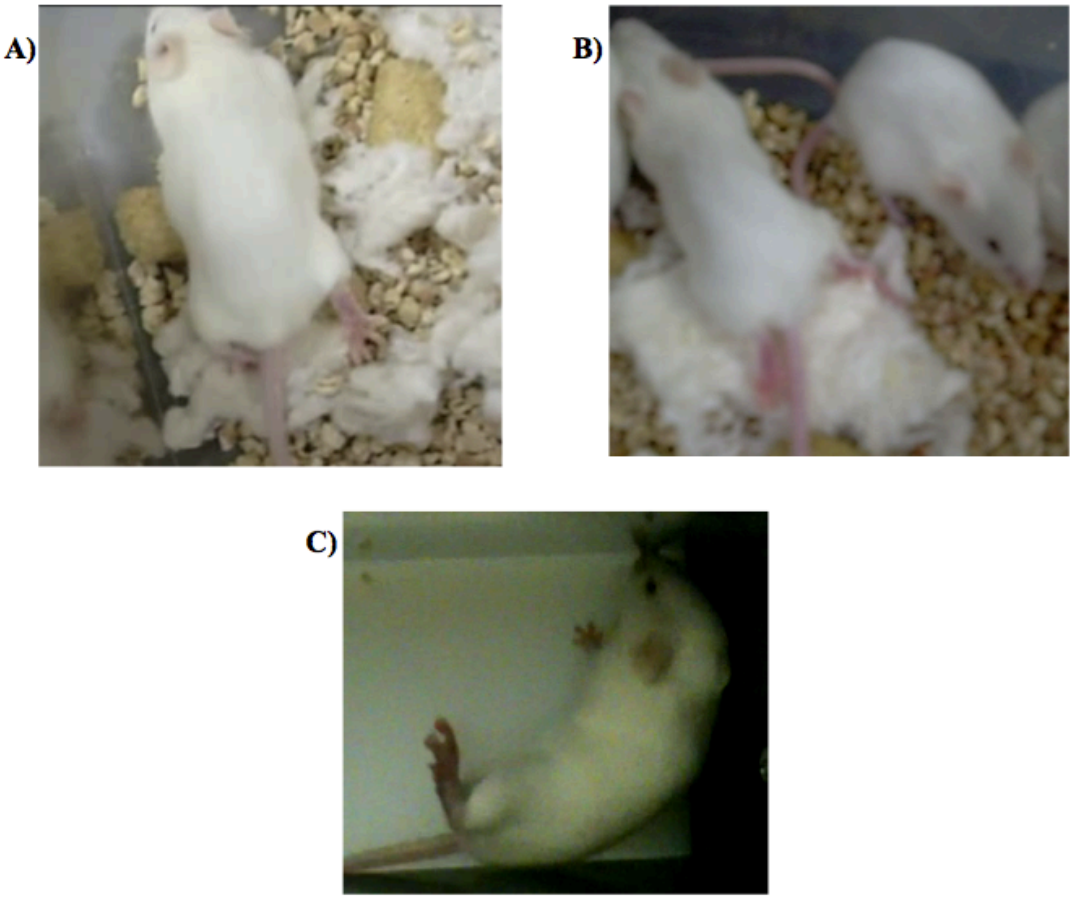

Figure 3-1: Paralytic attacks in HyperKPP mice. Paralytic attacks were observed when mice dragged one **A)** or both **B)** hind limbs behind their body while walking using their forelimbs. **C)** Paralysis was also observed when mice flip on their side. To verify the paralysis, HyperKPP mice were touched with a finger or pen: W.T. and un-paralyzed HyperKPP mice had the normal escape reaction, which was not observed in paralyzed HyperKPP mice.

TABLE 3-1

Age (months)	Total # of HyperKPP mice under observation	# of HyperKPP mice observed paralysed	Average # of days HyperKPP mice observed paralysed
0.75	6	1	0.2
1	7	6	3.2
2	8	2	1
3	10	0	-
4	9	0	-
6	6	0	-
9	4	2	0.2
12	5	2	0.6

Table 3-1: HyperKPP mice at the age of 1 month were observed paralyzed more frequently than any other age group. The table indicates the number of mice for which paralysis was observed and the average number of days these mice were observed paralyzed out of the five days of observation. The average number of days calculated included only mice for which paralysis was observed. Paralysis was observed as defined in Figure 3-1.

FIGURE 3-2

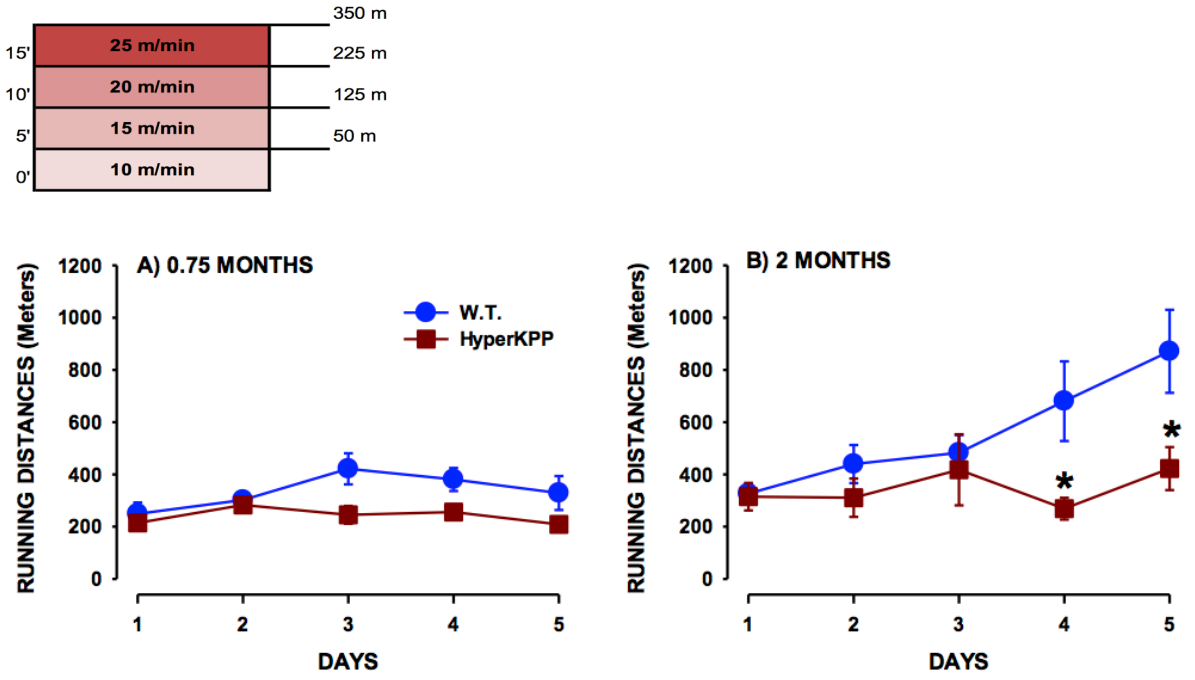

Figure 3-2: Two-month-old HyperKPP mice failed to improve their running capacity compared to W.T. mice. The graph shows the daily average running distance for W.T. and HyperKPP mice at A) 3 weeks of age and B) 2 months of age. Mice were elicited to run on treadmill with an uphill angle of 15° for 5 consecutive days. The initial speed was set at 10 m/min for 5 min and increased by 5 m/min every 5 min until the speed reached 25 m/min. Mice were removed from the treadmill when they could no longer maintain the required speed. The distances run by mice were calculated and used as an indication of exercise capacity. Vertical bars represent S.E. for 5-7 W.T. and HyperKPP mice.

* Mean distance run by HyperKPP mice was significantly different from the distance run by W. T mice.

ANOVA and L.S.D. $P < 0.05$

HyperKPP mice between 3 weeks and 12 months of age ran similar distances to W.T. mice on the first day of exercise, with average distances ranging between 214-314 m (Fig. 3-3A). Contrary to W.T., HyperKPP mice had a lower running capacity especially at 1-2 months of age on the fifth day of exercise. HyperKPP at these ages improved their running capacity by only 1.4-fold on the fifth day compared to the 2.6-fold achieved by W.T. mice. The large difference between W.T. and HyperKPP mice in the distance run on the fifth day decreased by 3 months of age when HyperKPP mice were able to improve as they ran 721 m compared to 934 m run by W.T. mice. By 4 months of age, HyperKPP mice ran a slightly longer distance (585 m) than their W.T. counterparts (511 m) on the fifth day of exercise. Interestingly, just like W.T. mice, HyperKPP mice at 3 weeks, 9 and 12 months of age failed to improve their running capacity on the fifth day (Fig. 3-3B).

Not all mice ran their longest distances on the fifth day. To verify that the differences between W.T. and HyperKPP mice observed on the fifth day were representative of the defect in HyperKPP mice; the maximum distances observed over the five days were also plotted for the different ages. Overall, the results were similar and the graph obtained (Fig. 3-3C) was a reflection of the fifth day results (Fig. 3-3B). On average, W.T. mice at the ages of 1 and 2 months ran longer distances than their HyperKPP counterparts and there was a tendency for HyperKPP mice to run slightly longer distances than W.T. mice at 4, 9, and 12 months of age (Fig. 3-3D).

Body weights were recorded before the exercise on the first day, to determine the possibility of body weight influence on exercise capacity. On average, there was no significant difference in weights between W.T. and HyperKPP mice in all age groups (Fig. 3-4).

FIGURE 3-3

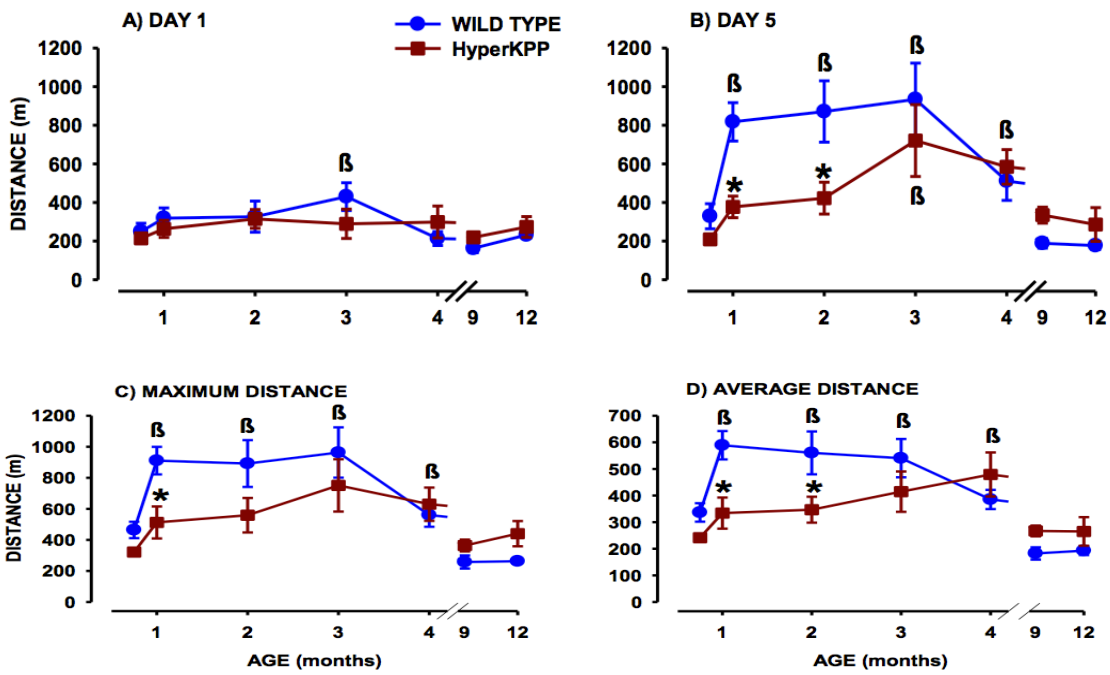

Figure 3-3: HyperKPP mice between 1-2 months of age ran significantly shorter distances than W.T. mice. Mice were elicited to run on treadmill with an uphill angle of 15° for 5 consecutive days. The initial speed was set at 10 m/min for 5 min and increased by 5 m/min every 5 min until the speed reached 25 m/min. Mice were removed from the treadmill when they could no longer maintain the required speed. The distances run by mice were calculated and used as an indication of exercise capacity. **A)** Distance run on the 1st day. **B)** Distance run on the 5th day. **C)** The maximum distance run. **D)** The average distance run over the five days of exercise. Vertical bars represent S.E. of 5-7 W.T. and HyperKPP mice.

β Mean distance run was significantly different from the distance at 3 weeks of age.

***** Mean distance run by HyperKPP mice was significantly different from the distance run by W. T mice.

ANOVA and L.S.D. $P < 0.05$.

FIGURE 3-4

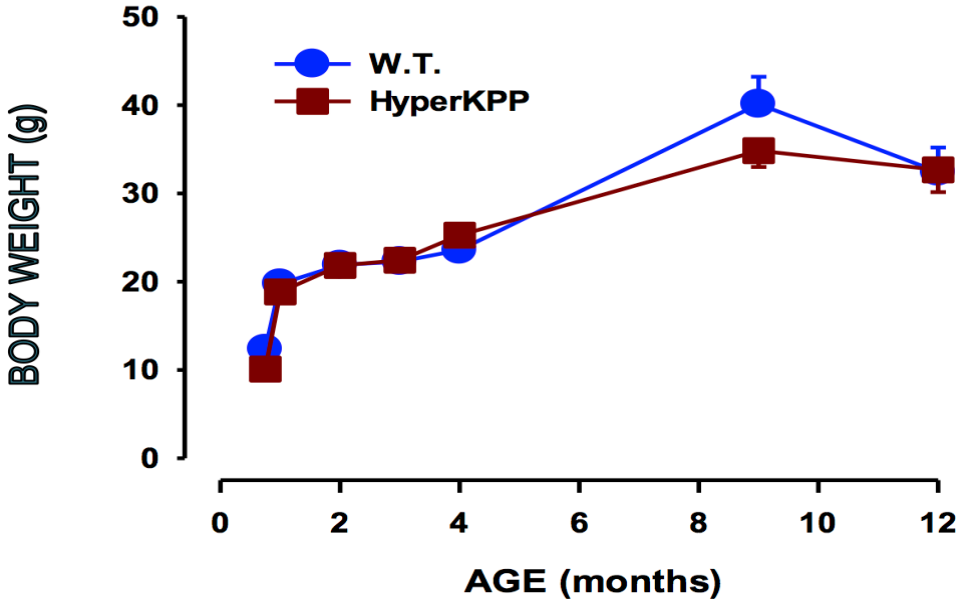

Figure 3-4: Body weights of exercising HyperKPP mice were not different from those of W.T. mice. Body weights were taken before the exercise session on day 1. Vertical bars represent S.E. of 5-7 W.T. and HyperKPP mice

No significant difference. ANOVA, $P > 0.05$.

MYOSIN EXPRESSION

As shown in previous studies, human patients[4] as well as Mouse[+/M1592V][7] have increased oxidative fibers in fast-twitch muscles associated with an increase in the number of fibers expressing fast oxidative MHC-IIA fibers. In this study, changes in fiber type content were assessed in EDL, soleus, diaphragm and FDB muscles and used as an index for changes in gene expression. In addition, both exercised and non-exercised groups were tested. The 5-day exercise protocol did not promote changes in fiber type composition in all muscles of W.T. mice as previously reported.[57] Therefore, for W.T., data from exercise and non-exercised mice were pooled together for all muscles.

EDL An average of 56 out of 1154 fibers (10%) stained positive for MHC-I fibers in 2-week-old W.T. EDL muscles and quickly diminished to 4% by 1 month and 2% by 2 months of age (Fig. 3-5A). After that, the level of MHC-I remained stable at ~2% until 12 months of age. In EDL of non-exercised HyperKPP mice, MHC-I content was similar to that of W.T. muscles. Although statistically not significant, there was a tendency for EDL of exercised HyperKPP mice to have a slightly higher level of MHC-I, exceeding the level of W.T. and non-exercised HyperKPP by 2-4% at 2,4 and 6 months of age. By 9-12 months, MHC-I content in EDL of exercised HyperKPP mice was similar to EDL of W.T. and non-exercised HyperKPP mice (Fig. 3-5A).

On average, MHC-IIA expression in W.T. EDL muscles remained consistent between 2 weeks and 12 months of age ranging between 13-23% (Fig. 3-5B). MHC-IIA content in HyperKPP EDL muscles was similar to that of W.T. for the first 3 weeks of life being 23% for W.T., 24% for non-exercised HyperKPP, and 16% for exercised HyperKPP.

However by 1.5 months of age, the number of fibers expressing MHC-IIA isoform increased from 26% at 1 month to 40% two weeks later in muscles of exercised HyperKPP mice. MHC-IIA expression reached a maximum of 57% by 2 months of age in EDL of exercised HyperKPP mice. There was no significant difference in the number of fibers expressing MHC-IIA between muscles of exercised and non-exercised HyperKPP mice until 3 months of age. At later ages, MHC-IIA expression in EDL of non-exercised mice decreased. At 4 and 6 months of age, there were 28% less fibers expressing MHC-IIA in EDL of non-exercised HyperKPP mice compared to muscles from exercised mice. By 9 and 12 month of age, MHC-IIA expression in EDL of exercised and non-exercised HyperKPP mice was still high compared to W.T. EDL.

MHC-IIB content in W.T. EDL muscles was initially 77% during the first 1.5 months of life before it decreased to 61% by 2 months and thereafter remained between 63% and 71% until 12 months of age (Fig. 3-5C). In EDL of non-exercised HyperKPP mice, MHC-IIB expression was significantly lower than W.T. muscles at 1, 4, 9 and 12 months of age, as 45-50% of the fibers expressed MHC-IIB isoform. The reduction was more pronounced in EDL of exercised mice. Compared to exercised mice, MHC-IIB expression was significantly higher in EDL of non-exercised mice at 2, 6, and 9 months of age. EDL muscles of non-exercised HyperKPP mice had 36%, 43% and 14% higher MHC-IIB content than muscles of exercised mice at 2, 6, and 9 months of age, respectively.

There were no significant differences observed in the expression of MHC-IIX in the EDL between the W.T., non-exercised & exercised HyperKPP mice (Fig. 3-5D). The number of fibers expressing MHC-IIX isoform ranged between 42%-69% in young mice until the age of 6 months, and 35%-46% in 9 and 12 months old mice.

The most pronounced changes in fiber type content in HyperKPP EDL muscles occurred for MHC-IIA and MHC-IIB fibers. While, on average, there was a clear increase in fibers expressing MHC-IIA and a decrease in fibers expressing MHC-IIB, a large variability was observed between HyperKPP EDL muscles so that not all HyperKPP animals showed a drastic change in fiber type content. Typically, EDL of adult W.T. mice express MHC-IIA in 12-17% of fibers, as reported previously.[66] Figure 3-6a shows a 2-month-old W.T. EDL muscle in which MHC-IIA was expressed in 21% of fibers. Between the ages of 2 and 12 months, three HyperKPP muscles -out of 48- showed MHC-IIA content within 10% of W.T. range (12-23%). The first one was from a 2-month old non-exercised mouse that expressed MHC-IIA in 18% of fibers (Fig. 3-6b). The second was from a 4-month non-exercised mouse and expressed MHC-IIA in 14% of fibers (picture not shown), and the last one was from a 12-month exercised mouse and expressed MHC-IIA in 23% of fibers (Fig. 3-6c). The majority of HyperKPP EDL muscles had MHC-IIA content higher than W.T. muscles, ranging between 30-71% (Fig. 3-6 d to g).

MHC-IIB content in HyperKPP EDL muscles was also affected but to a lower extent than that of MHC-IIA. Figure 3-7a shows an example of a W.T. EDL muscle with 57% MHC-IIB expression, which is within the range reported previously.[66] In HyperKPP muscles, MHC-IIB content was lower than that of W.T. mice of corresponding ages. Similarly, MHC-IIB content varied among HyperKPP EDL muscles. Seven HyperKPP EDL muscles out of 48 between 2 and 12 months of age showed a steep decrease in MHC-IIB content (17-27%) as shown in Figure 3-7 f and g. Six of the seven muscles were from the exercised group and distributed across the ages. Another nineteen animals showed a moderate decrease in MHC-IIB content (30-50%), eleven of which were from the exercised

group. The remaining HyperKPP EDL muscles (22 muscles) had MHC-IIB content similar to that of W.T. animals (51-86%), which is why the change in MHC-IIB content in HyperKPP muscles was not as drastic as that of MHC-IIA content (Fig. 3-7 b to e).

When the percentages of fibers expressing MHC-I, MHC-IIA, MHC-IIB, and MHC-IIX were added, the total for W.T. EDL varied between 119%-135% for mice between 1 and 12 months of age, except for 6-month-old mice for which the total was 147%. This is because some fibers, known as hybrids, express more than one MHC isoform.[67] Comparatively, the total increased to 133%-184% for EDL of non-exercised HyperKPP mice and to 118-168% for exercised mice, suggesting large increases in hybrid fibers.

When MHC-IIA and MHC-IIB content percentages were added in W.T. EDL muscles between 1 and 12 months of age, the sum was from 80%-86%. According to Banas et al[67], EDL muscles do not contain IIA/IIB hybrid fibers. In HyperKPP, however, the sum of MHC-IIA and MHC-IIB percentages ranged between 70% and 124% for muscles from non-exercised mice and between 87% and 108% for muscles from exercised mice between 1 and 12 months of age. Such elevated percentages of MHC-IIA and MHC-IIB fibers suggest that some HyperKPP EDL fibers may be IIA/IIB hybrids.

Similarly to IIA/IIB hybrids in W.T., the chance of IIA/IIX hybrids was low in W.T. EDL (54%-70%). The chance of IIA/IIX hybrids was also elevated in HyperKPP EDL compared to W.T EDL (Fig. 3-8). The sum of MHC-IIA and MHC-IIX percentages was 77%-105% for non-exercised HyperKPP mice and 84%-117% for exercised mice between 1 and 12 months of age. Only the sum of MHC-IIB and MHC-IIX percentages was similar and between 89%-130% for both W.T. and HyperKPP muscles.

FIGURE 3-5

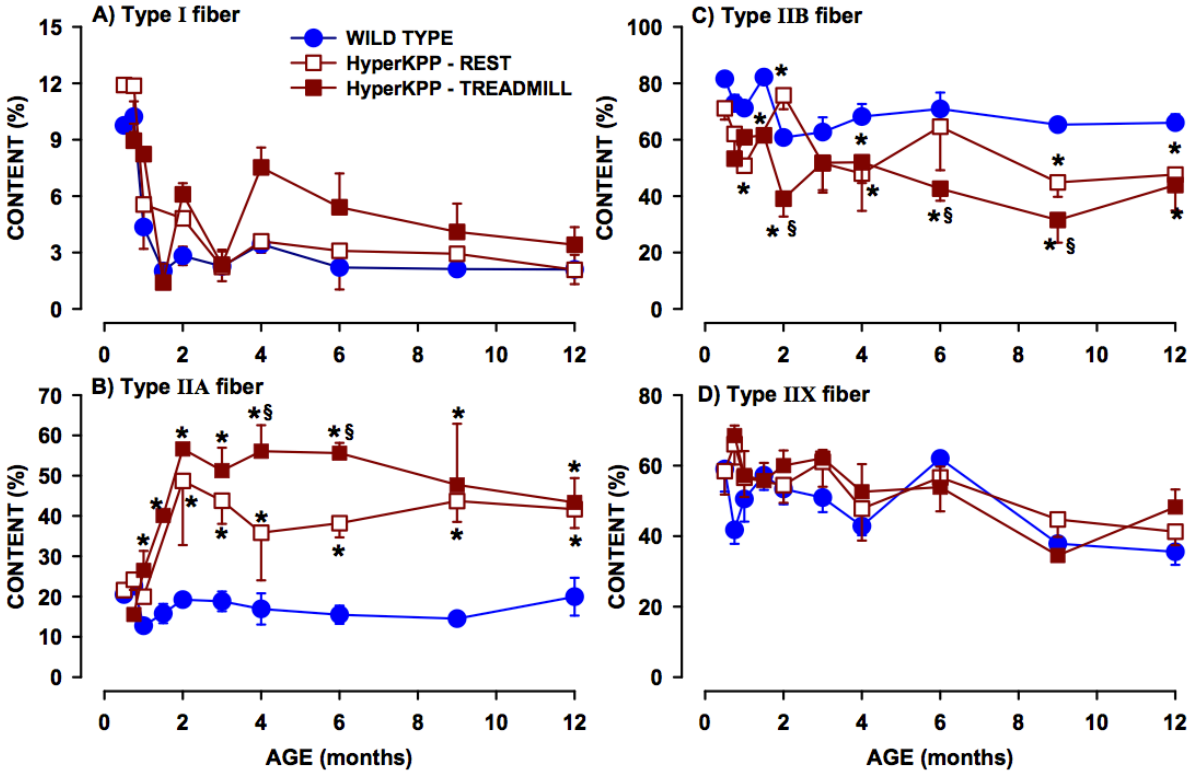

Figure 3-5: The number of fibers expressing MHC-IIA increased significantly while those expressing MHC-IIB decreased significantly in HyperKPP EDL muscles compared to W.T. EDL. Fiber types were determined using specific anti-MHC antibodies for type I (A), IIA (B), IIB (C) and IIX (D). Vertical bars represent the S.E. of 6-8 W.T. and HyperKPP mice.

* Significant difference between EDL of wild type and HyperKPP mice.

§ Significant difference between EDL of non-exercised and exercised HyperKPP mice.

ANOVA and L.S.D. $P < 0.05$.

FIGURE 3-6

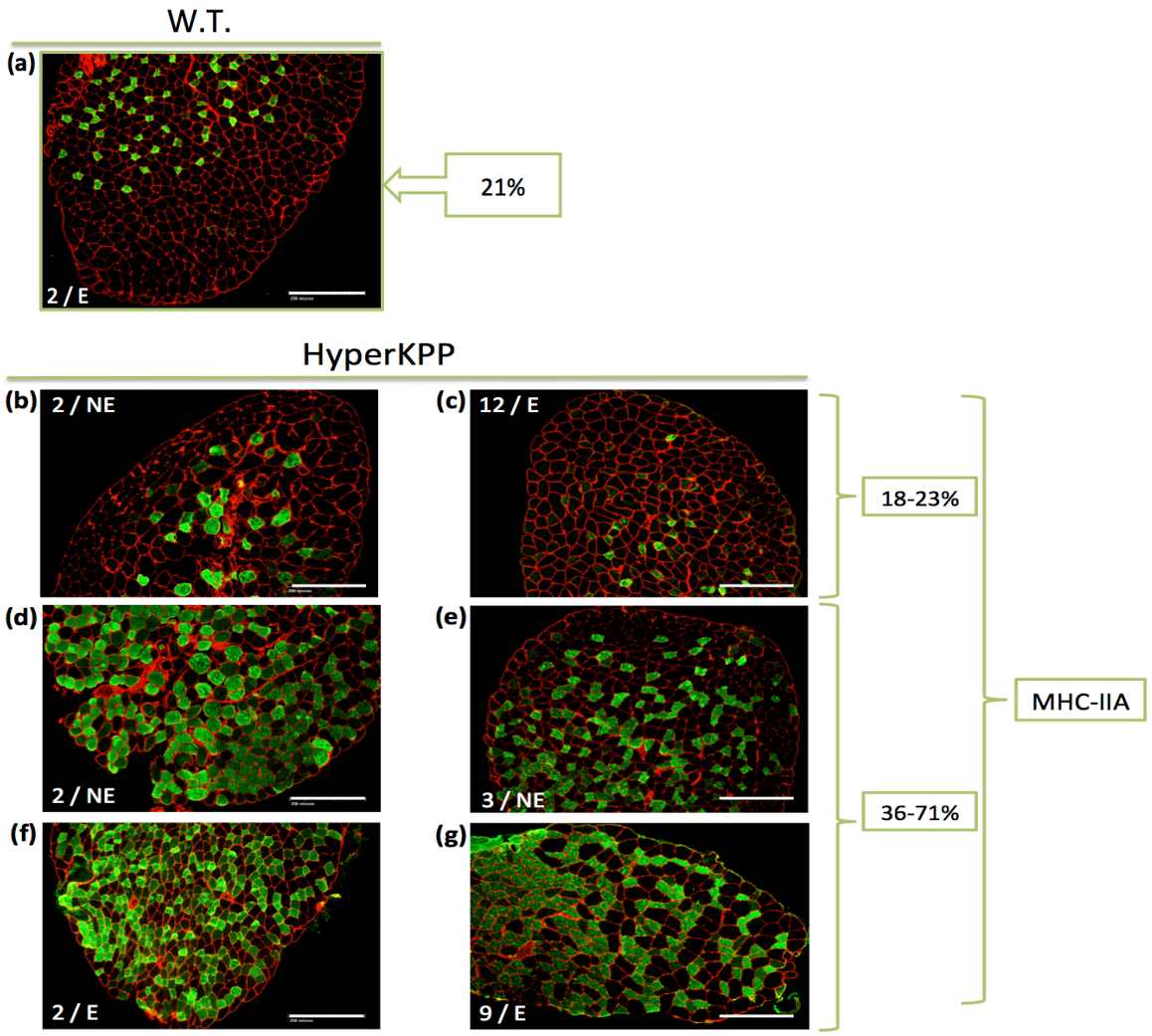

Figure 3-6: MHC-IIA expression was higher and more variable in HyperKPP EDL muscles compared to W.T. EDL muscles. EDL cross-sections were stained simultaneously with anti-laminin antibody (red), and MHC-IIA antibody (green). (a) An example of 2-month-old exercised W.T. EDL muscle. (b-g) Examples of variability in HyperKPP EDL muscles. All samples were from mice at ages in which the number of fibers expressing MHC-IIA was elevated (i.e. between 2 and 12 months of age). The numbers indicate: age of mouse (in months) / E: Exercised; NE: Non-Exercised. Bar=250 µm

FIGURE 3-7

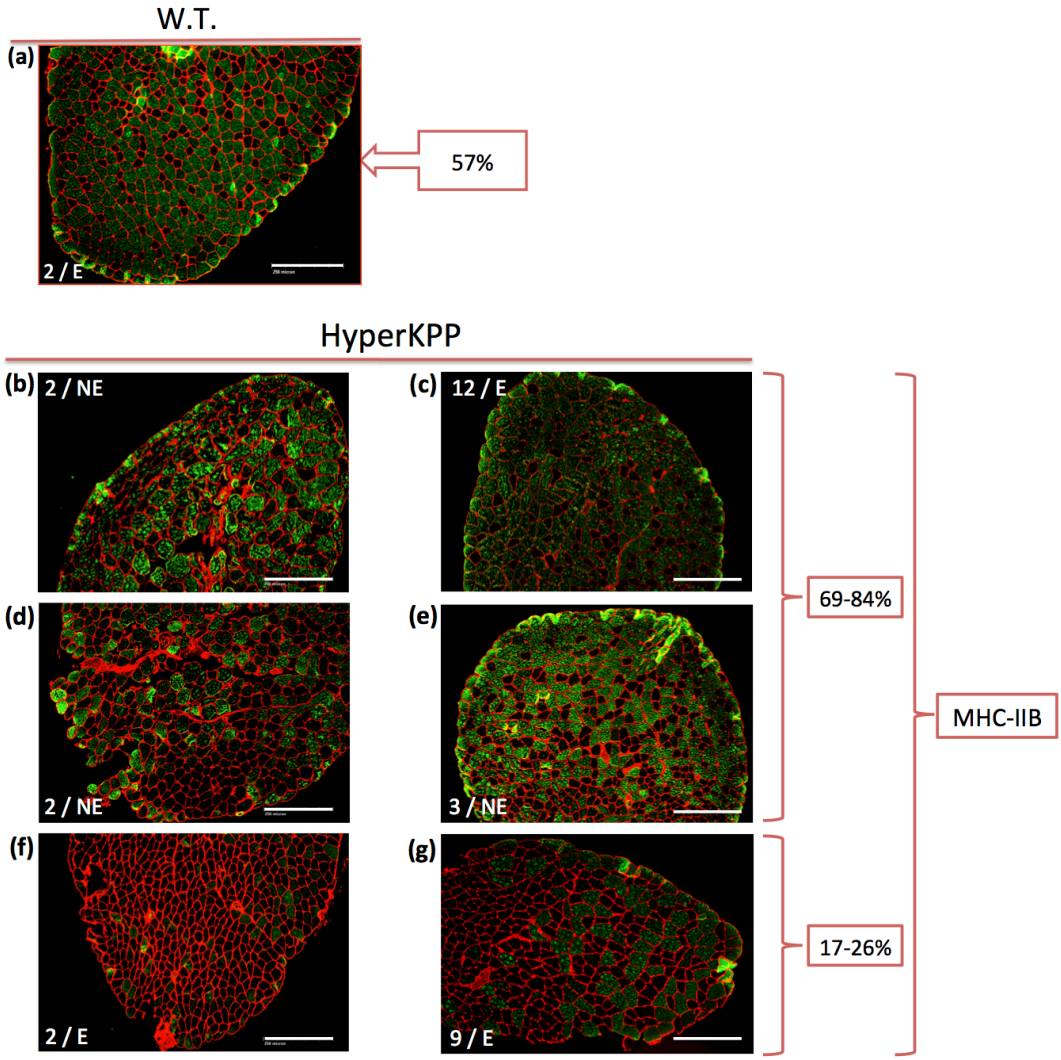

Figure 3-7: MHC-IIB expression was lower and more variable in HyperKPP EDL muscles compared to W.T. EDL muscles. EDL cross-sections were stained simultaneously with anti-laminin antibody (red), and MHC-IIB antibody (green). All cross-sections shown on this figure are from the same muscles as shown on Figure 3-6 and in the same order. (a) An example of 2-month-old exercised W.T. EDL muscle. (b-g) Examples of variability in HyperKPP EDL muscles. The numbers indicate: age of mouse (in months) / E: Exercised; NE: Non-Exercised. Bar=250 μm

FIGURE 3-8

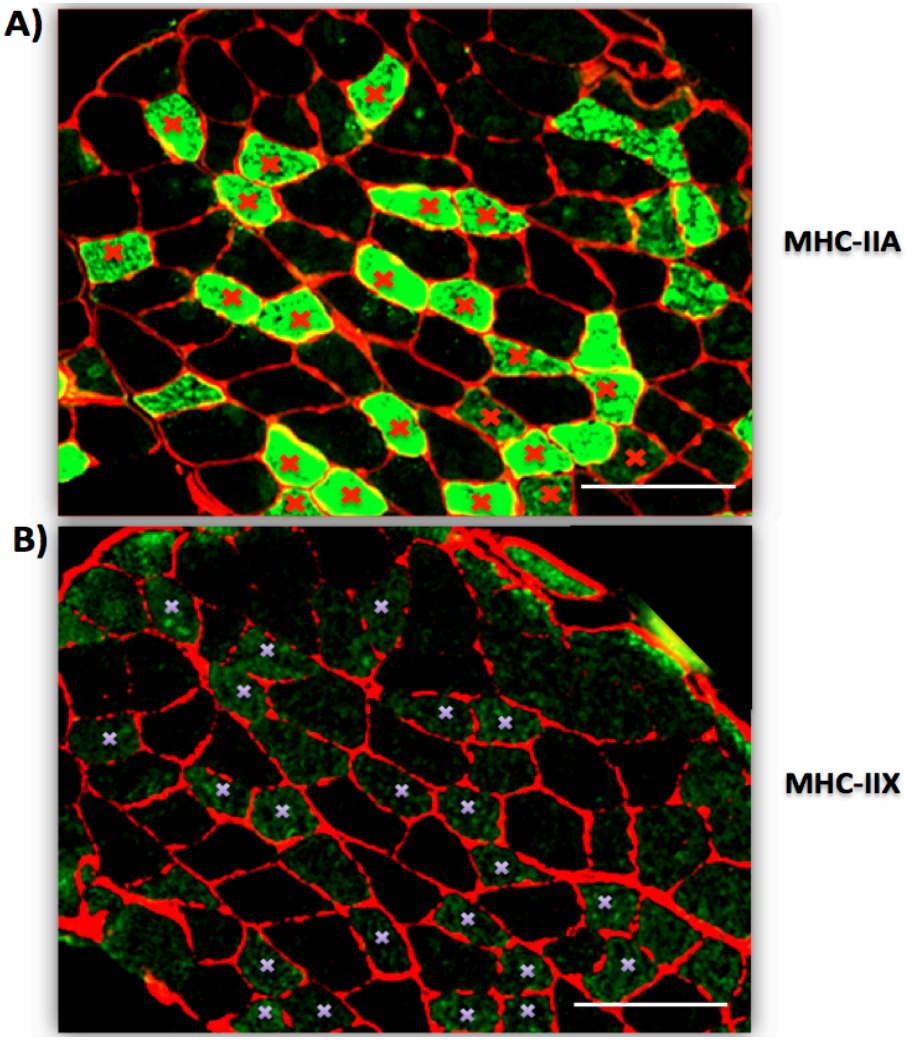

Figure 3-8: HyperKPP EDL muscles show an increased chance for IIA/IIX hybrids compared to W.T. EDL muscles. EDL serial cross-sections were stained simultaneously with anti-laminin antibody (red), and anti- MHC-IIA or MHC-IIX antibodies (green). (x) Signs indicate the same fibers stained with (A) MHC-IIA antibody, and (B) MHC-IIX antibody. Both cross-sections shown on this figure are from the same EDL muscle of a 3-month-old exercised HyperKPP mouse, and roughly from the same area of the muscle. Bar=100 μm

Soleus On average, MHC-I isoform was expressed in 50% of soleus fibers of 2-week-old W.T. mice (Fig. 3-9A). By 3 weeks of age, MHC-I was expressed in 61% of fibers and remained between 63-77% between 1-12 months of age. Unlike HyperKPP EDL muscles, exercise did not have any effect on the expression of MHC in HyperKPP soleus muscles so data were pooled. The number of fibers expressing MHC-I isoform in soleus of HyperKPP mice was similar to that of W.T. between 2 weeks and 2 months of age. At 2 weeks of age, 49% of HyperKPP soleus fibers expressed MHC-I. One week later it increased to 57% in 3-week-old mice, and reached 65% in 1.5 months old mice. At the age of 2 months, the number of fibers expressing MHC-I isoform in HyperKPP exceeded that in W.T. mice by 5%. The difference in content of MHC-I between W.T. and HyperKPP mice reached a maximum (14%) at 3 months of age. MHC-I expression in HyperKPP mice remained slightly higher than W.T. mice until 12 months of age

Similar to MHC-I, MHC-IIA was expressed in 47% in soleus of 2-week-old W.T. mice (Fig. 3-9B). It increased to 49% by 3 weeks but decreased to 40% by 1 month of age. It remained between 27% and 39% thereafter until 12 months of age. HyperKPP soleus muscles started with MHC-IIA content similar to that of W.T. between 2 weeks and 3 months of age, ranging between 33%-52%. However, differences became significant by 4 months of age when HyperKPP soleus muscles showed a consistent 10% decrease in fibers expressing MHC-IIA compared to W.T. muscles until 12 months of age.

Neither the W.T. nor HyperKPP soleus muscles expressed MHC-IIB (Fig. 3-9C). Furthermore, there was no difference observed in number of fibers expressing MHC-IIX isoform between soleus muscles of W.T. and HyperKPP mice (Fig. 3-9D). Both W.T. and HyperKPP muscles expressed a high level of MHC-IIX expression before the age of 1

month (50%-77%), and then gradually declined to about 30%-36% by 12 months of age.

Similar to their EDL muscles counterparts, HyperKPP soleus muscles showed variability in the expression of MHC types, although the variability was not as high as in the EDL muscles. Figure 3-10a shows a soleus muscle from a12-month-old non-exercised W.T. mouse with MHC-I expressed in 66% of fibers. Only one W.T. soleus muscle out of 49 between 1 and 12 months of age showed MHC-I expressed in over 90% of fibers at 9 months of age (picture not shown). Most HyperKPP soleus muscles (42 muscles out of 48) between 1 and 12 months of age expressed MHC-I in 60-83% of the fibers as seen in Figure 3-10b. Whereas six HyperKPP soleus muscles out of 48 -between 1 and 12 months of age- showed over 90% MHC-I expression (Fig. 3-10 c and d).

Figure 3-11 shows the same muscles in Figure 3-10 but stained with MHC-IIA instead. Figure 3-11a shows W.T. soleus muscle with MHC-IIA expressed in 38% of fibers, which represents the majority (27 out of 28) of muscles between 4 and 12 months of age. Only one W.T. soleus muscle -out of 28- showed MHC-IIA content below 15% at the age of 9 month (10% MHC-IIA content), compared to six HyperKPP soleus muscles -out of 30- that had MHC-IIA content below 15% (Fig. 3-11 c and d). The rest of the 30 HyperKPP muscles (24 muscles) had MHC-IIA expressed in 19-40% of fibers (Fig. 3-11b). Both exercised and non-exercised muscles showed average and extreme expressions.

FIGURE 3-9

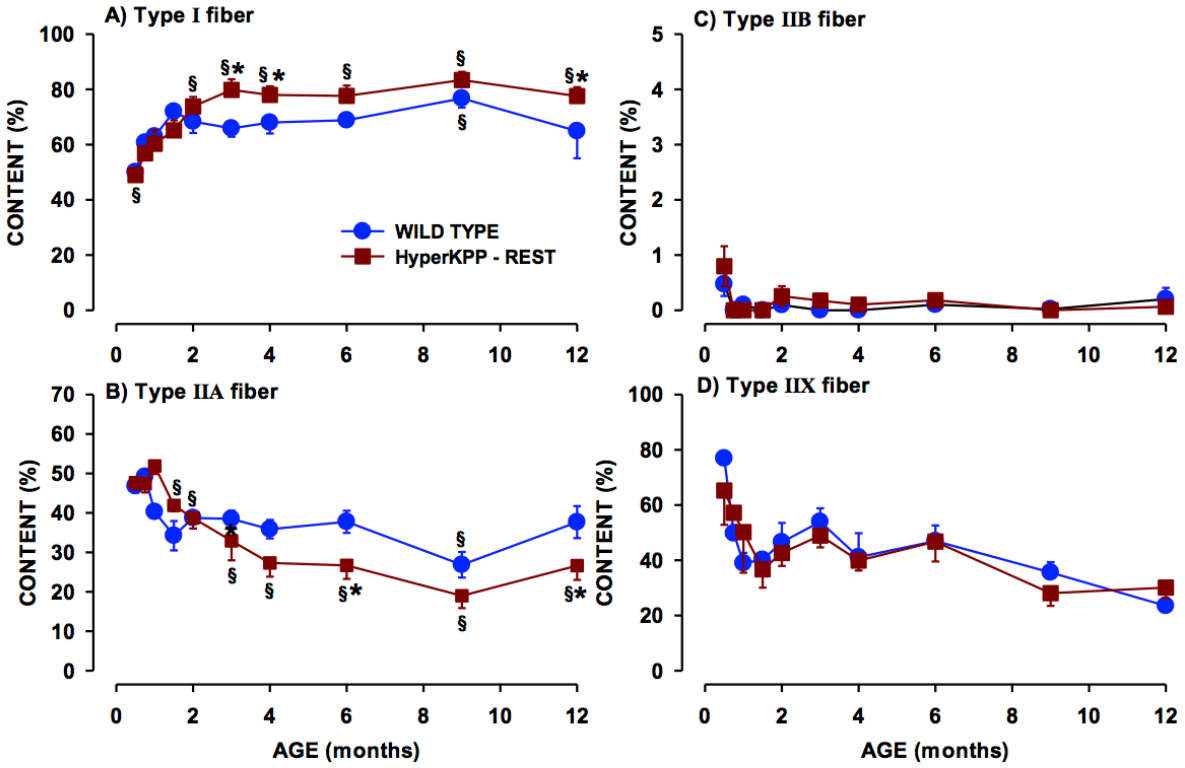

Figure 3-9: By 4 months of age, the number of fibers expressing MHC-I increased significantly in HyperKPP soleus while those expressing MHC-IIA decreased compared to W.T. soleus. Fiber types were determined using specific anti-MHC antibodies for type I (A), IIA (B), IIB (C) and IIX (D). Vertical bars represent the S.E. of 6-8 W.T. and HyperKPP mice.

* Significant difference between soleus of wild type and HyperKPP mice.

§ MHC content significantly different from content at 1 month of age.

ANOVA and L.S.D. $P < 0.05$.

FIGURE 3-10

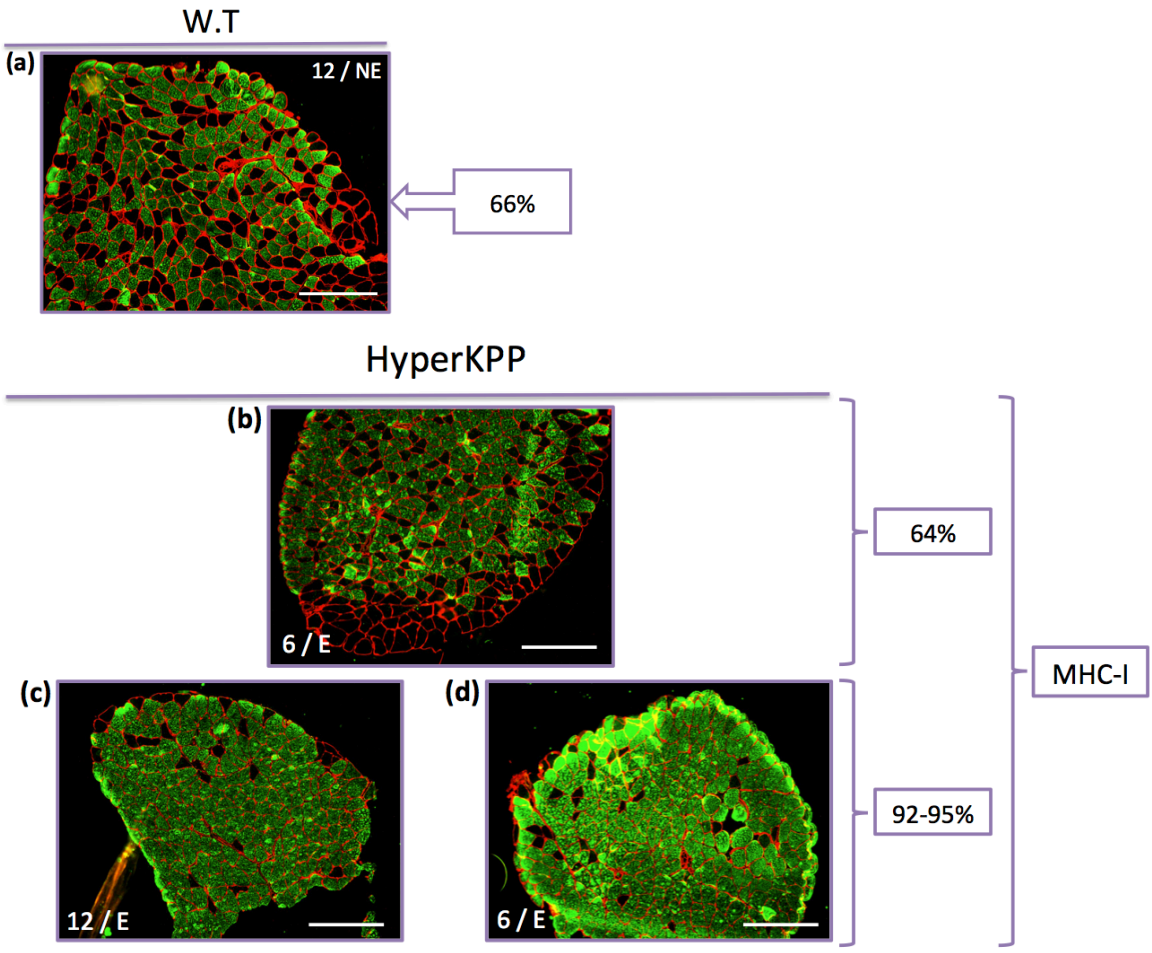

Figure 3-10: MHC-I expression in HyperKPP soleus muscles was increased and showed some variability, a feature that was not observed in W.T. muscles. Soleus cross-sections were stained simultaneously with anti-laminin antibody (red), and MHC-I antibody (green). (a) An example of 12-month-old non-exercised W.T. soleus muscle. (b-d) Examples of variability in HyperKPP soleus muscles. All samples were from mice at ages in which the number of fibers expressing MHC-IIA was reduced (i.e. between 4 and 12 months of age). The numbers indicate: age of mouse (in months) / E: Exercised; NE: Non-Exercised. Bar=250 µm

FIGURE 3-11

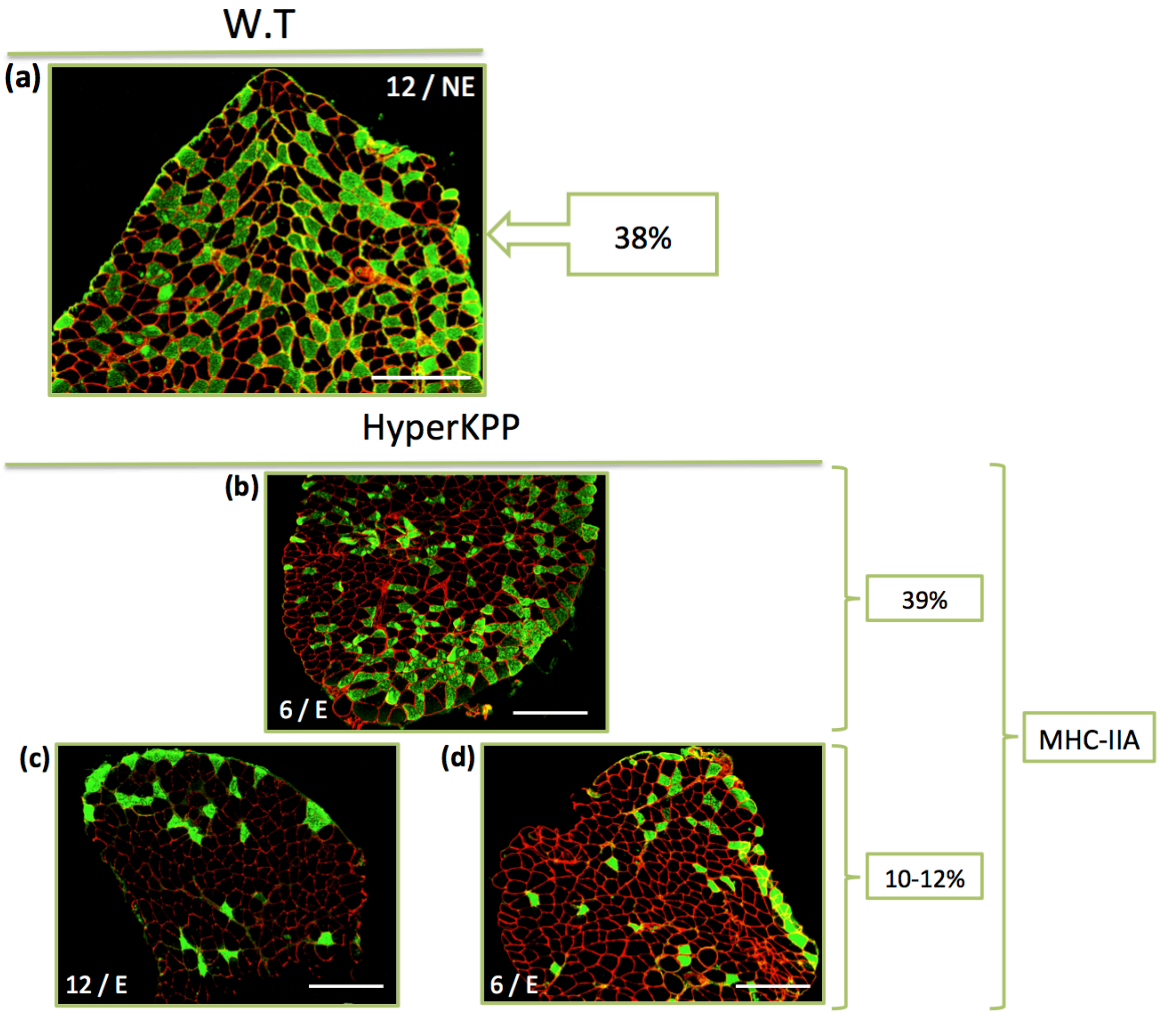

Figure 3-11: MHC-IIA expression in HyperKPP soleus muscles was decreased and also showed some variability, a feature that was not observed in W.T. muscles. Soleus cross-sections were stained simultaneously with anti-laminin antibody (red), and MHC-IIA antibody (green). All cross-sections shown on this figure are from the same muscles as shown on Figure 3-10 and in the same order. (a) An example of 12-month-old non-exercised W.T. soleus muscle. (b-d) Examples of variability in HyperKPP soleus muscles. The numbers indicate: age of mouse (in months) / E: Exercised; NE: Non-Exercised. Bar=250 µm.

Diaphragm and FDB:

Contrary to the EDL and soleus, no differences in fiber type composition were detected between the W.T. and HyperKPP diaphragm (Fig. 3-12) or FDB muscles (Fig. 3-13). Furthermore, for both muscles, exercise had no effect on fiber type composition and the data were pooled.

For both W.T. and HyperKPP diaphragm muscles, MHC-I content ranged between 9% and 12% until 12 months of age (Fig. 3-12A), while MHC-IIA content ranged between 33% and 39% for the first 3 weeks of life, and between 47%-71% until 12 months of age (Fig. 3-12B). MHC-IIB content was the lowest ranging between 0-10% between 2 weeks and 12 months of age. Exceptions were W.T. muscles at 3 weeks and 6 months of age, which were 15% and 9% higher than HyperKPP muscles, respectively (Fig. 3-12C). MHC-IIX content ranged between 50% and 65% for most W.T. and HyperKPP muscles until 12 months of age (Fig. 3-12D).

For both W.T. and HyperKPP FDB muscles, the fiber type composition was between 18% and 23% for MHC-I, 51% and 63% for MHC-IIA, 0.1% and 1% for MHC-IIB, and 51%-57% for MHC-IIX (Fig. 3-13).

FIGURE 3-12

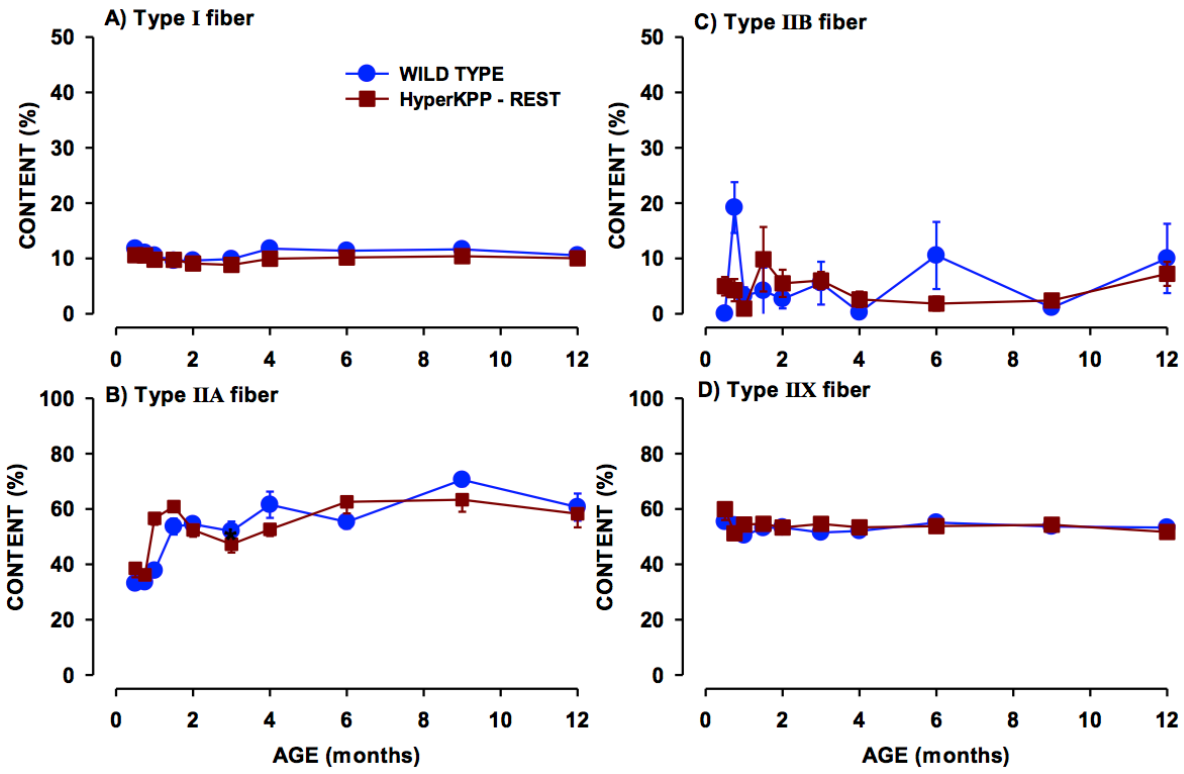

Figure 3-12: MHC fiber types content did not differ between W.T. and HyperKPP diaphragm muscles. Fiber types were determined using specific anti- myosin antibodies for type I (A), IIA (B), IIB (C), and IIX (D). Vertical bars represent S.E. of 6-8 W.T. and HyperKPP mice.

No significant difference. ANOVA, $P > 0.05$.

FIGURE 3-13

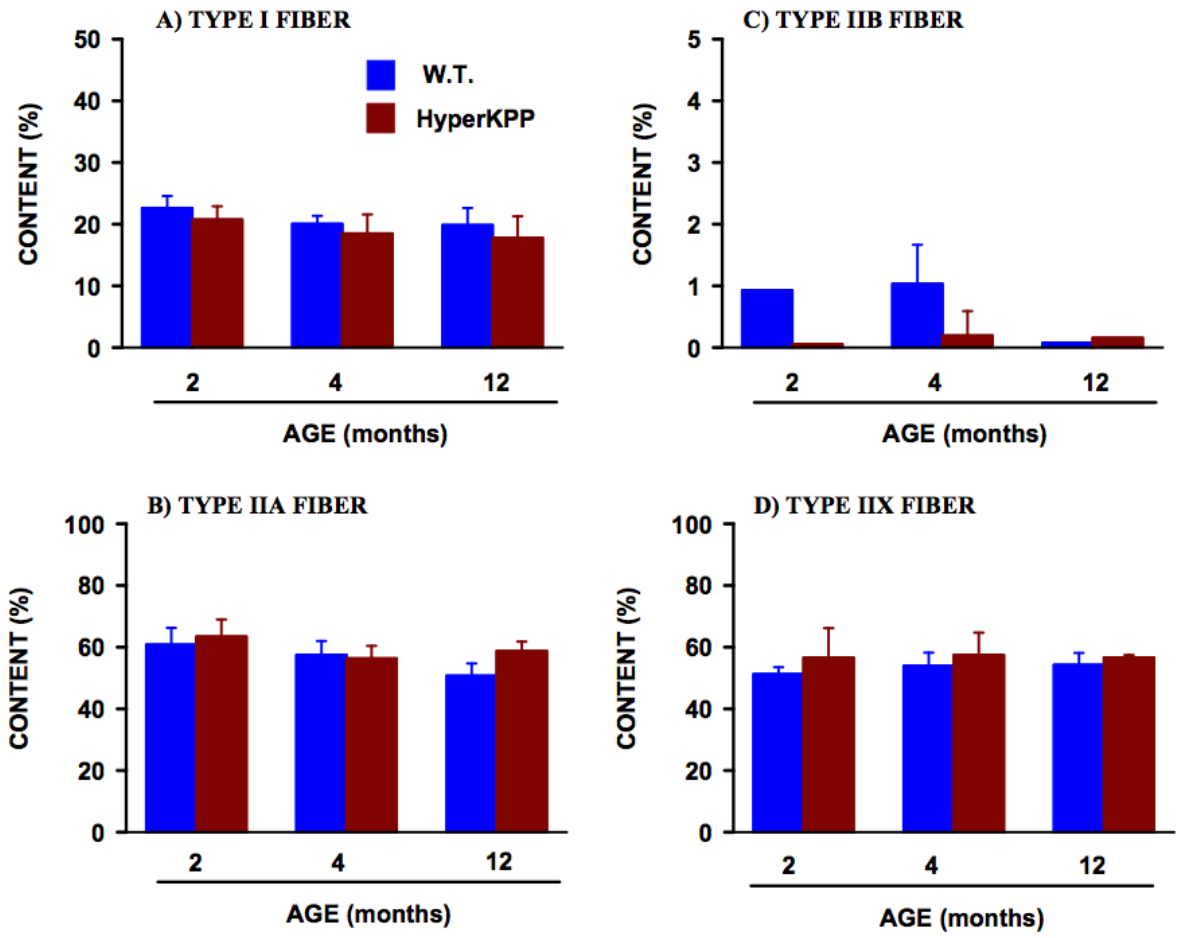

Figure 3-13: MHC fiber types content did not differ between W.T. and HyperKPP FDB muscles. Fiber types were determined using specific anti- myosin antibodies for type I (A), IIA (B), IIB (C), and IIX (D). Vertical bars represent S.E. 6-8 W.T. and HyperKPP mice.

No significant difference. ANOVA, $P > 0.05$.

FIBER DAMAGE

One of HyperKPP symptoms in humans that appear after middle age is muscle weakness caused by permanent, irreversible myopathy. The myopathy is marked by muscular atrophy, vacuolization, and central nuclei. In Mouse$^{(+/M1592V)}$, Hayward et al[7] observed a mild increase in the number of fibers with central nuclei by 4 months of age, whereas vacuolization was only observed in 2.8-month-old homozygotes. In this study, we examined younger and older 1 and 2 years old mice and investigated the effect of exercise on EDL, soleus, and diaphragm muscles. The results showed no difference in the extent of fiber damage between muscles of W.T. and HyperKPP or muscles of exercised and non-exercised mice.

In W.T. muscles, central nuclei were apparent by 12 months of age but only in 2% of EDL fibers in exercised and non-exercised mice (Fig. 3-15 and 3-14). In the soleus of exercised W.T. mice, 4% of fibers had central nuclei compared to the 2% observed in soleus muscles of non-exercised mice (Fig. 3-15). Similarly, in HyperKPP, central nuclei were apparent by 12 months of age in only 5% of EDL fibers in exercised and non-exercised mice (Fig. 3-14 and 3-15). Soleus muscles of exercised HyperKPP mice also had a slight elevation in the number of fibers with central nuclei (4%) compared to muscles of non-exercised HyperKPP mice (2%)(Fig. 3-15). Fibers with central nuclei were not observed in diaphragm muscles in any age group (data not shown). In addition, in older HyperKPP mice tested (23-24 months), EDL, soleus, and diaphragm muscles had very few fibers with central nuclei (data not shown). Therefore, no further analysis was carried out for age groups younger than 12 months. No vacuolization was observed in all sections tested.

FIGURE 3-14

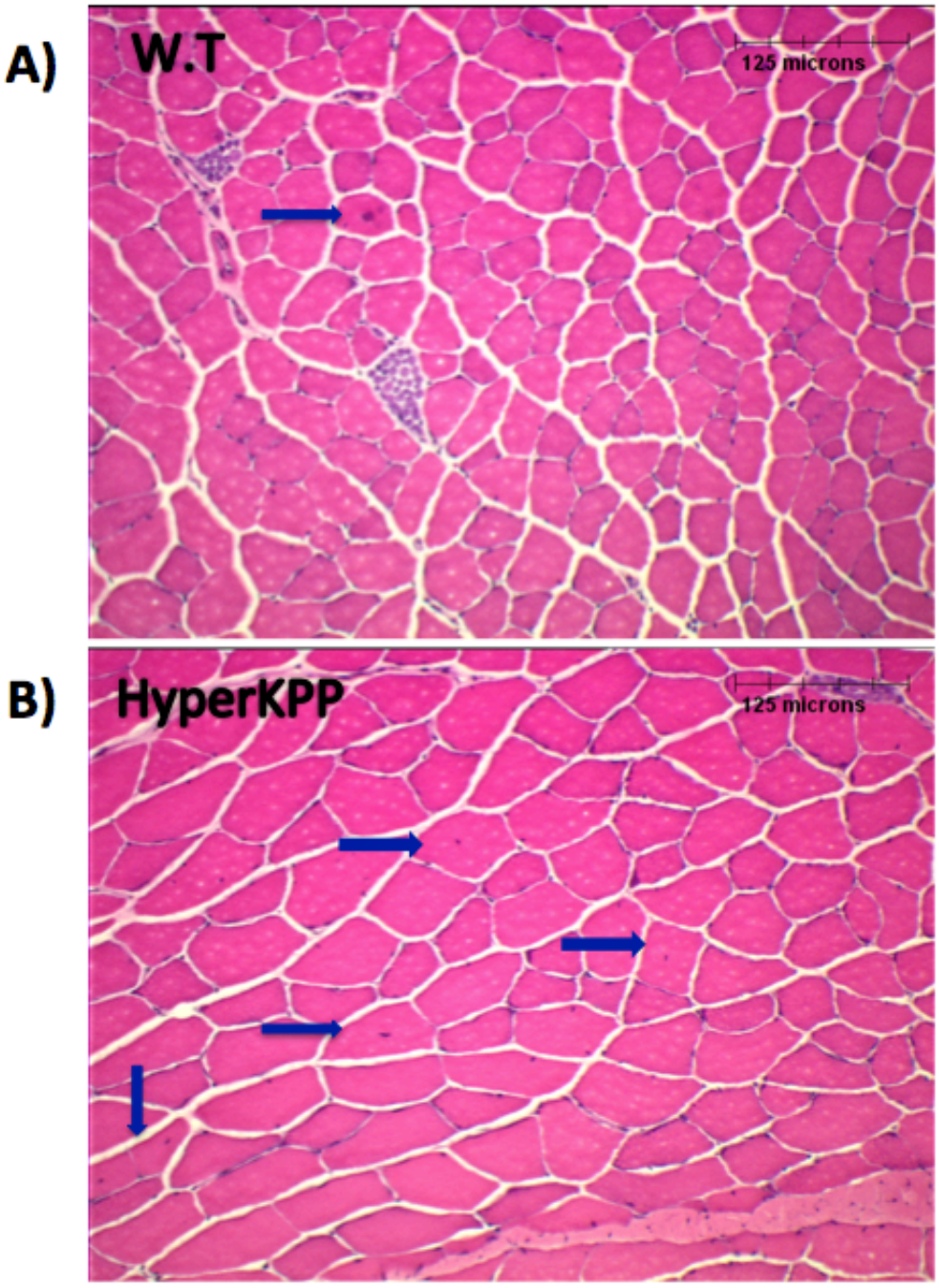

Figure 3-14: Muscle damage marked by central nuclei was not extensive in HyperKPP EDL muscles at 12 months of age. EDL cross-sections were stained with Hematoxylin and Eosin. A) W.T. EDL muscle. B) HyperKPP EDL muscle. Bar= 125 µm

FIGURE 3-15

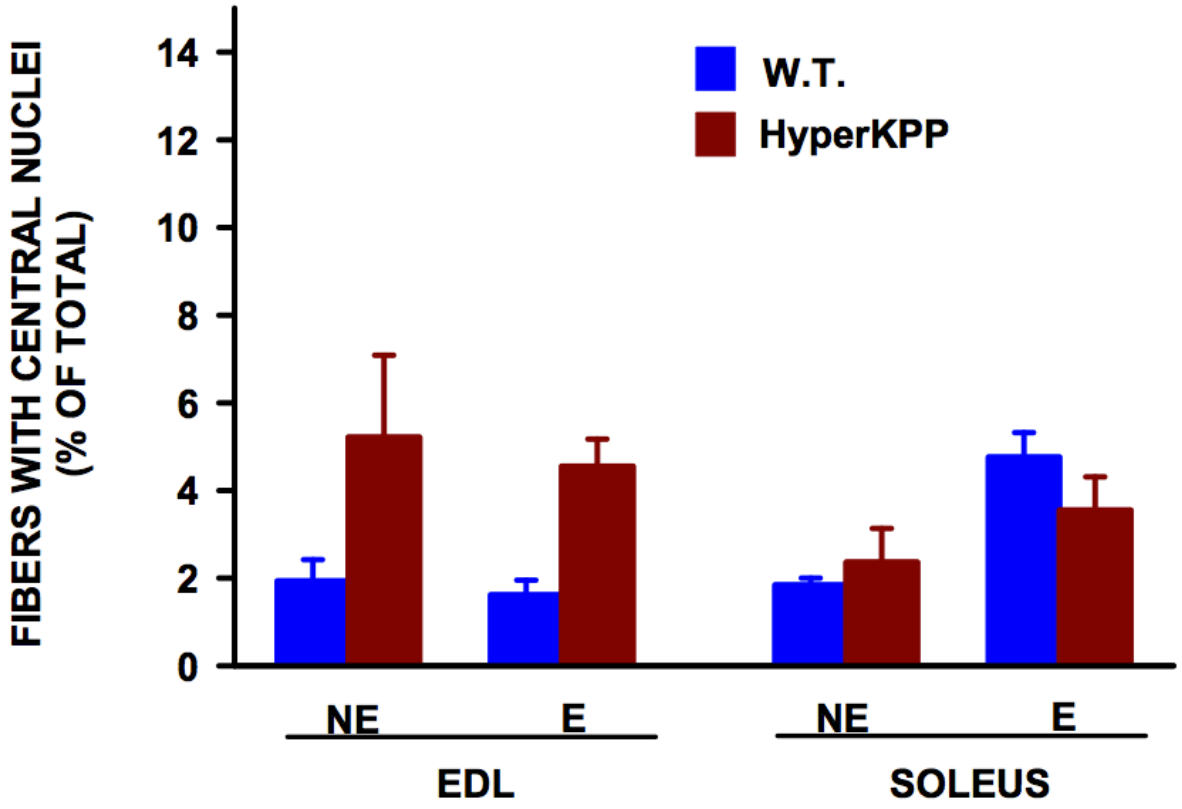

Figure 3-15: Muscle damage marked by central nuclei was not extensive in EDL and soleus muscles of HyperKPP mice at 12 months of age. EDL and soleus cross-sections were stained with Hematoxylin and Eosin. The total number of fibers with central nuclei was manually counted and expressed as a percentage of the total number of fibers. Vertical bars represent S.E. 6 W.T. and 10 HyperKPP mice.

No significant difference. ANOVA, $P > 0.05$.

CHAPTER 4

DISCUSSION

The major findings of this study were: (1) paralytic attacks were observed in HyperKPP mice especially at 1 and 2 months of age; (2) HyperKPP mice between 1-2 months of age had a lower exercise capacity than their W.T. counterparts; (3) there was an increase in fibers expressing MHC-IIA isoform in HyperKPP EDL as early as 2 months of age, and an increase in fibers expressing MHC-I in HyperKPP soleus by 4 months of age; (4) HyperKPP diaphragm and FDB muscles did not show changes in fiber type composition; and (5) fiber damage in Mouse$^{(+/M1592V)}$ was mild and no vacuolization was observed.

PARALYSIS IN Mouse$^{(+/M1592V)}$

In their 2008 study, Hayward et al[7] did not report paralysis in Mouse$^{(+/M1592V)}$. Therefore, this was the first study reporting paralysis in Mouse$^{(+/M1592V)}$. Unlike W.T. mice, paralyzed HyperKPP mice failed to escape when touched with a pencil. Therefore, the observations of mice dragging their hind limbs while moving using forelimbs, and mice flipping on their sides, were interpreted as paralysis. While EMG measurements will clearly indicate paralysis by the absence of electrical activity, for this study, the event of paralysis was confirmed by checking the escape reaction.

The observation of paralysis also showed that the attacks were brief. Even at the age of 1 month -time of highest frequency- paralysis was not observed in all mice or in the same mouse daily over the five days of observation. Perhaps the observation time spent during treadmill running was long enough to visualize those paralytic attacks reported, which could

be missed if not observed over a long period of time.

EXERCISE PERFORMANCE

At the age of 3 weeks, exercise capacity of W.T. mice did not improve over the five days of exercise, and the average distance run was lower compared to mice at 1 and 2 months of age. These young mice are possibly still in the process of developing their motor abilities and thus struggle to improve. According to Mänttäri et al[68], action potential conduction velocity increased gradually in a pattern similar to the increase in $Na_{V1.4}$ content during development in mice, in which $Na_{V1.4}$ content reached a maximum by 25 days after birth.

The average distance run by W.T. FVB mice in this study was similar to averages reported in previous studies examining FVB mice. For example, 2-month-old W.T. mice in this study ran an average of 560 m. Similarly, Massett et al[69] reported an average of 625 m run on treadmill by 2-month-old FVB mice.

Despite the short period of exercise in this study (5 days), W.T. mice between 1 and 3 months of age were able to improve their running capacity throughout the five days of exercise by at least 2.2 fold. Although mice from different strains vary in their exercise capacities, these results were in agreement with Thabet et al[66] findings that showed 2-month-old C57 mice improving their running capacity by 2.5 folds over five days of treadmill running. The rapid increase in exercise capacity was due to the beneficial effects of short-term exercise on muscles. Baar et al[70] showed that even a short-term exercise, five daily bouts of swimming in their case, was enough to enhance respiratory capacity of 3-month-old rats. Furthermore, mRNA of transcriptional co-activator PGC-1α (enhances

oxidative metabolism of muscles and promotes mitochondrial biogenesis) was increased by 50% after only three days of exercise and by twofold after five days of exercise. Consequently, exercise performance improved with enhanced respiratory capacity of the muscle.[70, 71]

At 4 months of age, W.T. mice had a lower running improvement over the five days of exercise. On average, they also ran shorter distances compared to mice between 1 and 3 months of age. Furthermore, 9 and 12-month-old W.T. mice failed to improve their running capacity over the five days of exercise and on average ran the shortest distances among their younger peers. This progressive loss of exercise capacity in older mice is expected and could be attributed to aging.[72-74] In a previous study on rats between 2 and 12 months of age, it was found that rats between 2 and 4 months of age had the highest running activity, followed by rats between 5 and 9 months of age, while those between 10 and 12 months of age had the lowest running activity compared to younger rats.[72]

There are many factors behind the loss of exercise capacity with age. It has been suggested that age-related morphological changes at the level of the neuromuscular junction may alter exercise capacity in aged mammals.[74, 75] Ultrastructural studies on adult young and old mice (between 3 and 24 months of age) showed a decrease in presynaptic terminals, a decrease in synaptic vesicles, and a decrease neurotransmitter release in old mice compared to young ones.[75] In addition to structural changes, studies have also shown that VO_2 max and maximal exercise capacity declined with age in untrained C57 mice. This was supported by other studies showing a significant decrease in mitochondrial count with age in mice. [75, 76]

Compared to their W.T. littermates, HyperKPP mice at 3 weeks of age ran similar

distances during the five days of exercise. However, between 1-2 months of age, HyperKPP mice ran shorter distances on the fifth day of exercise, which was reflected on the lower average performance compared to W.T. mice. The differences in exercise performance between W.T. and HyperKPP mice cannot be attributed to body weights since both groups were similar in that aspect. However, the presence of myotonic discharges in HyperKPP mice could be responsible for the lower exercise capacity in these mice. In a recent study by Dejong and Renaud (unpublished results), EMG measurements of gastrocnemius muscles showed a significantly higher electrical activity *in vivo* in HyperKPP between 2 weeks and 2 months of age compared to W.T. mice while at rest or actively moving. Such activity was indicative of myotonic discharges. Therefore, myotonic discharges may have lowered the exercise capacity of HyperKPP mice between 1-2 months by starting the fatigue process sooner in these mice. The increase in muscle contraction frequency caused by myotonic discharges may have increased the demand for ATP. In such cases, muscle fibers tend to initiate the onset of fatigue to protect against ATP depletion by reducing Ca^{2+} release from the sarcoplasmic reticulum (SR). This in turn leads to the drop in force observed in the fatigue process. In addition, myotonic discharges lead to an increase in both $[Na^+]_i$ and $[K^+]_e$, which work synergistically to induce the process of fatigue by lowering action potential amplitude and reducing Ca^{2+} release from the SR.[77, 78]

HyperKPP mice between 4 and 12 months of age had a slightly better exercise performance than their W.T. counterparts. The increase in fibers expressing oxidative MHC-IIA observed in HyperKPP muscles could be the reason behind the improved exercise endurance. It was reported in several studies that the exercise-induced increase in oxidative fibers contribute to improved exercise performance.[70, 79] However, the large increase in

fibers expressing MHC-IIA isoform observed in fast-twitch EDL of HyperKPP mice should have led to a bigger improvement in exercise performance than what was observed. In a study performed on C57 mice, a 1.3-fold increase in running distance was accompanied by a 2-fold increase in MHC-IIA fibers in fast-twitch plantaris muscles (Waters, 2004). In this study, EDL of HyperKPP mice between 4 and 12 months of age had a 3.1-fold increase in fibers expressing MHC-IIA isoform compared to W.T. mice. Such an increase should have been accompanied by at least a 2-fold increase in running distance. Instead, only 1.4-fold increase was observed in distances run by these mice, indicating a running defect. It is possible that the myotonic discharges were still affecting HyperKPP mice at these ages, restricting their exercise performance despite the increase in oxidative fibers.

MYOSIN EXPRESSION

EDL and soleus muscles: Shifts towards MHC-IIA and MHC-I

Fiber type composition of FVB mice used in this study showed a considerable agreement with the results reported using C57 and CD-1 mice.[66, 67] In previous studies, an increase in oxidative MHC-I fibers was reported in fast-twitch muscles of HyperKPP patients (Bradley, 1990) and an increase in MHC-IIA fibers was reported in fast-twitch tibialis anterior muscle (TA) of 12-month-old HyperKPP mice.[4, 7] Hayward et al[7] also reported an increase in PGC-1α in fast-twitch HyperKPP muscles, indicating an increase in oxidative capacity. This study also reports a drastic increase in fibers expressing MHC-IIA in EDL of HyperKPP mice by 1.5 months of age, followed by a decrease in fibers expressing MHC-IIB isoform. In the soleus of HyperKPP mice, there was an increase in MHC-I followed by a decrease in MHC-IIA isoform by 4 months of age.

Such changes in fiber types have been well documented in the literature studying myotonic channelopathies such as myotonia congenita and potassium aggravated myotonia

(PAM) that are caused by mutations in the ClC-1 and $Na_{V1.4}$, respectively. Genetically modified mice with myotonia showed a clear reduction in MHC-IIB that was compensated for by an increase in MHC-IIA fibers in the TA muscles.[80] It was also suggested that the hyper-excitability of myotonic muscles resulted in biochemical adaptations similar to those observed in chronic low-frequency stimulated muscles.[81] Additionally, studies have shown that stimulating EDL muscles of rats with soleus-like motor activity (low frequency stimulation) induced significant changes in fiber type composition by increasing MHC-IIA fibers and decreasing MHC-IIB content.[55, 82] On the other hand, soleus muscles showed smaller changes in fiber type content (a decrease in MHC-IIA and a small increase in MHC-I) when exposed to the same pattern of stimulation. And since soleus muscles already express slow MHC-I in more than 75% of fibers, low-frequency stimulation affects it in a minimal way. [82] In HyperKPP, myotonic discharges resemble low-frequency stimulation, thus HyperKPP muscles were able to adapt their fiber type composition to meet the myotonic demands.

Fiber type transition is considered one of the slowest and most complex outcomes of changes at the level of gene expression. Calabria et al[83] suggested a mechanism by which this transition may occur. It involved different recruitment patterns of Nuclear Factor of Activated T cells (NFAT) family, which have been linked to slow fibers and oxidative capacity of the muscle. Their results showed that the four NFAT isoforms: NFATc1, NFATc2, NFATc3, and NFATc4 were present in skeletal muscles; however, their activation pattern determined the MHC isoform expressed in the muscle. They showed that slow stimulation induced the expression of MHC-I, which required all NFAT isoforms to be activated. Whereas MHC-IIA and MHC-IIX expression needed the activation of NFATc2,

NFATc3, and NFATc4. The expression of MHC-IIB required the activation of only NFATc4. They also showed that continuous slow stimulation increased $[Ca^{2+}]_i$ which activated Ca^{2+}-calcineurin pathway, leading to an increase in oxidative fibers in the muscle. Therefore, it is possible that the myotonic discharges in HyperKPP increased the activation of NFATc2, NFATc3, and NFATc4 via Ca^{2+}-calcineurin pathway in EDL muscles promoting the expression of MHC-IIA isoform. While in the soleus, myotonic discharges may have cause the activation of all four NFAT isoforms, promoting the expression of MHC-I.

The exercise effect. The 5-day exercise protocol was not enough to exert changes on fiber type composition in W.T. animals. This was expected, as TA muscles of C57 mice did not show changes in fiber type composition even after five weeks of treadmill running.[66] Exercise also did not have an effect on fiber type composition in soleus, diaphragm or FDB muscles of HyperKPP mice. However, in the EDL of HyperKPP mice, exercise seemed to exacerbate the increase in MHC-IIA and decrease in MHC-IIB isoforms observed compared to muscles of non-exercised mice. In EDL of HyperKPP mice, exercise may have been reinforcing the intensity of the stimulation already taking place as a result of myotonic discharges.

Hybrids. When percentages of the four MHC isoforms were summed in this study, the total number was increased in HyperKPP as compared to W.T. muscles. This is an indication of an increase in hybrid fibers, which result from a sequential transformation between the fiber types.[54] According to Banas et al[67], 17% of fibers in EDL muscles of CD-1 mice expressed MHC-IIA isoform and 57% expressed MHC-IIB, but IIA/IIB hybrids were not observed in these muscles. However, it was reported that myotonia could cause

fiber type transitions that give rise to such rare IIA/IIB hybrids.[81] This might also be occurring in HyperKPP since there was an increase in the sum of MHC-IIA and MHC-IIB contents in HyperKPP EDL muscles compared to W.T. muscle.

There was also an increase in the sum of MHC-IIA and MHC-IIX contents in HyperKPP compared to W.T. muscles suggesting a higher chance for IIA/IIX hybrids in EDL muscles of HyperKPP mice (Fig. 3-8). This indicates that the drastic increase in fibers expressing MHC-IIA isoform in EDL of HyperKPP muscles does not necessarily reflect an increase in pure MHC-IIA fibers, but instead is caused by the increase in IIA/IIX hybrids.

Diaphragm and FDB muscles: Unaffected

One of the main objectives of this study was to examine how different muscles in HyperKPP were affected *in vivo* by examining changes in fiber types. This study reported that the most drastic changes in fiber type composition occurred in EDL, followed by soleus muscles. These results agreed with *in vitro* contractility experiments, which showed that EDL of HyperKPP mice muscles had the most contractile dysfunction followed by soleus muscles (Lucas, M.Sc. thesis). The results also showed that the fiber type compositions of the diaphragm and FDB muscles were not affected in HyperKPP mice, supporting the second hypothesis. This further suggests that the extent of changes in fiber type *in vivo* may reflect the severity of symptoms in these muscles. In fact, *in vitro* studies showed minimal contractile dysfunction in the diaphragm as well as FDB muscles, which was supported by *in vivo* results from this study.

SEVERITY OF SYMPTOMS IN MUSCLES IN RELATION TO $Na_{V1.4}$ CONTENT AND ACTIVITY

Some of the differences in the severity of symptoms between the four muscles tested in this study could be related to their fiber type composition, $Na_{V1.4}$ channel content and activity.

Most of the changes in fiber type composition in HyperKPP were reported in fast-twitch muscles such as the EDL and the TA.[4, 7] These muscles mostly express fast-glycolytic MHC-IIB and MHC-IIX isoforms. Other muscles such as soleus, the diaphragm and FDB muscles expressed a minimal amount of MHC-IIB fibers, which could explain the low effect on these muscles.

It was expected that the extent of severity of HyperKPP symptoms in different muscles was proportional to $Na_{V1.4}$ channels content: The greater the content, the more severe the symptoms. Western blot experiments investigating $Na_{V1.4}$ content in different HyperKPP muscles showed that $Na_{V1.4}$ content was highest in EDL muscles, while the soleus expressed only 32% of the $Na_{V1.4}$ channels content observed in EDL muscles (Ammar and Renaud, unpublished results). This was not surprising since EDL muscles were more affected *in vivo* and *in vitro* than soleus muscles. FDB muscles also had a small $Na_{V1.4}$ channel content (23% of $Na_{V1.4}$ content in EDL). This also goes with the lack of symptoms in this muscle. However, the diaphragm, which was neither affected *in vivo* nor *in vitro*, had a high $Na_{V1.4}$ channel content (76% of $Na_{V1.4}$ content in EDL).

Another discrepancy was observed with Na^+ influx through $Na_{V1.4}$ channels in HyperKPP muscles. It was expected that Na^+ influx would be highest in EDL followed by

soleus muscles. However, Na^+ influx in the EDL of HyperKPP mice was very similar to that of soleus muscles (270 nmoles / g wet weight / min for EDL vs. 265 for soleus) (Renaud lab, unpublished results). On the other hand, HyperKPP FDB muscles had the lowest Na^+ influx (24 nmoles / g wet weight / min), which was expected due to the lack of changes in these muscles. Surprisingly, the highest influx was observed in diaphragm (323 nmoles / g wet weight / min), adding to the mystery of this muscle. Table 4-1 summarizes the differences between muscles reported in this project (Renaud lab, unpublished results).

Taking all parameters into account, the severity of symptoms in EDL, soleus and FDB muscles in HyperKPP could be correlated to their respective $Na_{V1.4}$ channel contents, and Na^+ influx. However, when taking into account the diaphragm muscle, the high $Na_{V1.4}$ channel content and high Na^+ influx observed in this muscle does not explain how it is unaffected and spared from paralysis, contractility defects, and fiber type changes. These results suggest that the diaphragm may have special protective mechanisms since it is constantly active. This activity may act like mild exercise as it prevents paralysis in humans.[19] Unfortunately, the mechanism behind this protective feature is not well understood.

FIBER DAMAGE

The presence of fiber damage and vacuolar myobathy in HyperKPP patients is well established in the literature.[4, 22] In Mouse$^{(+/M1592V)}$, Hayward et al[7] reported a mild increase in fibers with central nuclei in the hamstring muscle at 4 months of age. They also reported an increase in fibers with central nuclei in the TA muscles of 24-month-old HyperKPP mice, with vacuolization reported in homozygote but not heterozygote HyperKPP mice. In this study, a mild increase in fibers with central nuclei in HyperKPP was observed in 12 and 24-

month-old mice. Therefore, this study further supports Hayward et al[7] findings with respect to the mild fiber damage observed in Mouse$^{(+/M1592V)}$ muscles and the lack of vacuolization.

TABLE 4-1

Differences	Highest				Lowest
Changes in fiber typs	EDL	>>	Soleus >	Diaphragm ~	FDB
Contracility defects	EDL	>	Soleus >>	Diaphragm ~	FDB
$Na_{V1.4}$ content	EDL	>	Diaphragm >	Soleus ~	FDB
Na^+ influx	Diaphragm	>	EDL ~	Soleus >>	FDB

Table 4-1: Different muscles were affected to different extents in HyperKPP mice. The EDL muscle of HyperKPP mice showed the most changes in fiber type composition and had the most contractile dysfunction. FDB muscles on the other extreme were the least affected by HyperKPP. The lack of effect on the diaphragm muscle of HyperKPP cannot be explained by $Na_{V1.4}$ channel content or activity.

HUMAN VS MOUSE$^{(+/M1592V)}$

Mouse$^{(+/M1592V)}$ was considered a good animal model to study HyperKPP because it presented many HyperKPP characteristics that were seen in HyperKPP patients such as the myotonic discharges and muscle force depression at high $[K^+]_e$, *in vitro*.[7] In addition, and as seen in this study, Mouse$^{(+/M1592V)}$ also presented paralysis. However, while some HyperKPP mice were observed paralyzed, many did not present paralysis suggesting a high variation in the severity of HyperKPP symptoms between mice. Immunohistochemical analysis also revealed a high variability in fiber type composition among HyperKPP mice especially in EDL muscles. Similarly, variability in symptoms was observed between human HyperKPP subjects even within the same family.[18, 84, 85] It was suggested that differences between patients (and hence between HyperKPP mice) might be due to variations in defective-to-normal $Na_{V1.4}$ ratio in heterozygotes.[18]

In addition, variation was observed within the same subject. The observation of paralysis in this study showed that the same HyperKPP mouse was not observed paralyzed daily during the five days of observation. This was also seen in clinical studies, in which the same patient might or might not experience paralysis after exercise.[86] McManis et al[86] related the differences within the same patient to fluctuations in electrolyte balance and status within the muscle.

Although both HyperKPP patients and Mouse$^{(+/M1592V)}$ present paralysis and variability in symptoms, differences were observed with respect to the characteristics of the paralysis itself, reflecting major differences between Mouse$^{(+/M1592V)}$ and human patients *in vivo*. One of these differences is rest after strenuous exercise being a common trigger for

paralytic attacks in HyperKPP patients. Miller et al[5] reported that rest after strenuous exercise triggered paralytic attacks in 80% of all HyperKPP patients tested, and in 73% of patients with the M1592V mutation. However, in Mouse$^{(+/M1592V)}$, paralysis was randomly observed before, during, or after exercise with no apparent correlation. In addition, paralytic attacks in patients with M1592V mutation lasted on average between 24 and 144 hours. In Mouse$^{(+/M1592V)}$, however, the attacks were brief lasting between 10 and 30 seconds.

Another difference between human patients and Mouse$^{(+/M1592V)}$ is the extent of fiber damage. Vacuolization was not observed in Mouse$^{(+/M1592V)}$, whereas in humans it was observed in many cases. One explanation for the mild damage in HyperKPP mice could be the short life span of mice compared to humans. Mice may not live long enough to experience extensive fiber damage.

SUMMARY

The main objective of this project was to follow the progression of HyperKPP in Mouse$^{(+/M1592V)}$ in relation to $Na_{V1.4}$ channel content and/or activity. Particularly to determine if the asymptomatic period at the beginning of life, and the onset of symptoms result only from the defect in $Na_{V1.4}$ channels and not from changes in the expression of other ion channels as a result of changes in gene expression.

$Na_{V1.4}$ channel content reached a maximum at 3 weeks in W.T.[17, 68] as well as in HyperKPP mice (Ammar and Renaud, unpublished results). At 2 weeks of age, HyperKPP EDL had a Na^+ influx that was 3.6-times greater than wild type EDL (Barbalinardo and Renaud, unpublished results). These results explain the contractile defects observed *in vitro* in EDL muscles of 2-week-old HyperKPP mice. The results also suggest that the paralysis, which peaked in HyperKPP mice 1 week after $Na_{V1.4}$ channel content reached a maximum,

as well as the defect in exercise capacity that started at 1 month of age, were possibly due to the increase in $Na_{V1.4}$ channel content and reaching a critical level by 3 weeks of age.

The results in this project do not support, but also do not eliminate, the possibility of the involvement of changes in other membrane components that may trigger or increase the severity of symptoms. Such changes would be the result of changes in gene expression, which occurred later between 1.5-2 months of age in HyperKPP mice, manifested in the changes in fiber types observed in the EDL. As a result, direct measurements of channel activity and content are necessary.

In conclusion, the results from this study as well as from the *in vitro* studies performed for this project support the hypothesis that the defect in $Na_{V1.4}$ channels is the only factor responsible for the onset and progression of symptoms. However, this study demonstrated that differences between muscles in HyperKPP were not just dependent on $Na_{V1.4}$ channel content or activity. Therefore, these differences cannot be related only to the defect in $Na_{V1.4}$ channels in HyperKPP.

REFERENCES

1. Hayward LJ, Sandoval GM, Cannon SC. Defective slow inactivation of sodium channels contributes to familial periodic paralysis. Neurology, 1999. 22;52(7):1447-53.

2. Cannon SC. From mutation to myotonia in sodium channel disorders. Neuromuscular Disorders, 1997. 7: 241-249

3. Gamstorp I, Hauge M, Helweg-Larsen HF, Mjones H, Sagild U. Adynamia Episodica Hereditaria. A disease clinically resembling familial periodic paralysis but characterized by increasing serum potassium during the paralyitic attacks. The American Journal of Medicine, 1957. 4;23:385-90.

4. Bradley WG, Taylor R, Rice DR, Hausmanowa-Petruzewicz I, Adelman LS, Jenkison M, Jedrzejowska H, Drac H, Pendlebury WW. Progressive myopathy in hyperkalemic periodic paralysis. Archives of Neurology, 1990. 47(9):1013-7.

5. Miller TM, Dias da Silva MR, Miller HA, Kwiecinski H, Mendell JR, Tawil R, McManis P, Griggs RC, Angelini C, Servidei S, Petajan J, Dalakas MC, Ranum LP, Fu YH, Ptácek LJ. Correlating phenotype and genotype in the periodic paralyses. Neurology, 2004. 63(9):1647-55.

6. Jurkat-Rott K, Lehmann-Horn F. Genotype-phenotype correlation and therapeutic rationale in hyperkalemic periodic paralysis. Neurotherapeutics, 2007. 22;4:216-24.

7. Hayward L, Kim J, Lee M, Zhou H, Kim J, Misra K, Salajegheh M, Wu F, Matsuda C, Reid V, Cros D, Hoffman E, Renaud J, Cannon S, Brown R. Targeted mutation of mouse skeletal muscle sodium channel produces myotonia and potassium-sensitive weakness. J Clin Invest, 2008. 118 (4):1437-1449.

8. Ashcroft FM. Ion Channel and Disease California: Academic Press; 2000.

9. Fill M, Copello JA. Ryanodine receptor calcium release channels. Physiological Reviews. [Review]. 2002, 01;82(4):893-922.

10. Steinmeyer K, Ortland C, Jentsch TJ. Primary structure and functional expression of a developmentally regulated skeletal muscle chloride channel. Nature. [Comparative Study]. 1991, 28;354(6351):301-4.

11. Kubo Y, Baldwin TJ, Nung Jan Y, Jan LY. Primary structure and functional expression of a mouse inward rectifier potassium channel. Nature. [Article], 1993. 11;362(6416):127-33.

12. Fakler B, Brändle U, Glowatzki E, Weidemann S. ScienceDirect.com - Cell - Strong voltage-dependent inward rectification of inward rectifier K^+ channels is caused by intracellular spermine. Cell, 1995. 80(1):149-154.

13. Dwyer TM. The permeability of the endplate channel to organic cations in frog muscle. The Journal of General Physiology, 1980. 01;75(5):469-92.

14. Catterall WA. Structure and function of voltage-gated ion channels. Annual review of biochemistry, 1995. 64:493-531.

15. Cannon S. Pathomechanisms in channelopathies of skeletal muscle and brain. Annu Rev Neurosci, 2006. 1;29:387-415.

16. Barchi R. Molecular Pathology of the Skeletal Muscle Sodium Channel - Annual Review of Physiology, 1995. 57(1):355.

17. Zhou J, Hoffman EP. Pathophysiology of sodium channelopathies. Studies of sodium channel expression by quantitative multiplex fluorescence polymerase chain reaction. J Biol Chem, 1994. 269(28):18563-71.

18. Zhou J, Spier SJ, Beech J, Hoffman EP. Pathophysiology of sodium channelopathies: correlation of normal/mutant mRNA ratios with clinical phenotype in dominantly inherited periodic paralysis. Human Molecular Genetics, 1994. 3(9):1599-603.

19. Carson M, PEARSON CM. Familial hyperkalemic periodic paralysis with myotonic features. The Journal of pediatrics, 1964. 64:853-865

20. Ebers GC, George AL, Barchi RL, Ting-Passador SS, Kallen RG, Lathrop GM, Beckmann JS, Hahn AF, Brown WF, Campbell RD. Paramyotonia congenita and hyperkalemic periodic paralysis are linked to the adult muscle sodium channel gene. Annals of neurology, 1991. 30(6):810-6.

21. Lehmann-Horn F, Rüdel R, Ricker K, Lorković H, Dengler R, Hopf HC. Two cases of adynamia episodica hereditaria: in vitro investigation of muscle cell membrane and contraction parameters. Muscle Nerve, 1983. Feb 1;6(2):113-21.

22. Person CM. The periodic paralyses: Differential features and pathological observations in permanent myopathic weakness. Brain : a journal of neurology, 1964. Jul 01;87:341-54.

23. Goldin AL, Barchi RL, Caldwell JH, Hofmann F, Howe JR, Hunter JC, Kallen RG, Mandel G, Meisler MH, Netter YB, Noda M, Tamkun MM, Waxman SG, Wood JN, Catterall WA. Nomenclature of voltage-gated sodium channels. Neuron. [Letter], 2000 Nov 01;28(2):365-8.

24. Yoshimura T, Kaneuji M, Okuno T. European Journal of Pediatrics, Volume 140, Number 4 - SpringerLink. European Journal of Pediatrics, 1983. 140(4):338-343.

25. Stühmer W, Conti F, Suzuki H, Wang XD, Noda M, Yahagi N, Kubo H, Numa S. Structural parts involved in activation and inactivation of the sodium channel. Nature, 1989 Jul 22;339(6226):597-603.

26. Catterall WA. Molecular properties of voltage-sensitive sodium channels. Annual review of biochemistry. [Review]. 1986; 55:953-85.

27. Kallen RG, Cohen SA, Barchi RL. Structure, function and expression of voltage-dependent sodium channels. Molecular Neurobiology, 1993 Sep;7(3-4):383-428.

28. Noda M, Shimizu S, Tanabe T, Takai T, Kayano T, Ikeda T, Takahashi H, Nakayama H, Kanaoka Y, Minamino N, Kangawa K, Matsuo H, Raftery MA, Hirose T, Inayama S, Hayashida H, Miyata T, Numa S. Primary structure of Electrophorus electricus sodium channel deduced from cDNA sequence. Nature, 1984 Nov 08;312(5990):121-7.

29. Ji S, Sun W, George AL, Horn R, Barchi RL. Voltage-dependent regulation of modal gating in the rat SkM1 sodium channel expressed in Xenopus oocytes. The Journal of General Physiology. [Comparative Study]. 1994 Oct 01;104(4):625-43.

30. Sheets MF, Hanck DA. Gating of skeletal and cardiac muscle sodium channels in mammalian cells. The Journal of physiology. [Comparative Study]. 1999 Feb 15;514 (Pt 2):425-36.

31. Hodgkin AL, Huxley AF. A quantitative description of membrane current and its application to conduction and excitation in nerve. The Journal of physiology, 1952 Aug 01;117(4):500-44.

32. Hayward LJ. Inactivation defects caused by myotonia-associated mutations in the sodium channel III-IV linker. The Journal of General Physiology, 1996 Jun 01;107(5):559-76.

33. Hayward LJ, Brown RH, Cannon SC. Slow inactivation differs among mutant Na channels associated with myotonia and periodic paralysis. Biophysical Journal, 1997 Apr 01;72(3):1204-19.

34. Vilin YY, Ruben PC. Slow Inactivation in Voltage-Gated Sodium Channels: Molecular Substrates and Contributions to Channelopathies. Cell Biochemistry and Biophysics, 2001;35(2):171-90.

35. Cummins TR, Sigworth FJ. Impaired slow inactivation in mutant sodium channels. Biophysical Journal, 1996 Jul 1;71(1):227-36.

36. Catterall WA. Voltage-dependent gating of sodium channels: correlating structure and function. Trends in Neurosciences1986;9:7-10.

37. Vassilev PM, Scheuer T, Catterall WA. Identification of an intracellular peptide segment involved in sodium channel inactivation. Science (New York, NY). [In Vitro]. 1988 Sep 23;241(4873):1658-61.

38. West JW, Patton DE, Scheuer T, Wang Y, Goldin AL, Catterall WA. A cluster of hydrophobic amino acid residues required for fast Na(+)-channel inactivation. Proceedings of the National Academy of Sciences of the United States of America. [Comparative Study]. 1992 Nov 15;89(22):10910-4.

39. Featherstone D, Richmond J. ScienceDirect.com - Biophysical Journal - Interaction between fast and slow inactivation in Skm1 sodium channels. Biophysical Journal, 1996. 71:3098-3109

40. Cha A, Ruben P, George A, Fujimoto E. Domains III and IV, but Not I and II, Are Immobilized by Na+ Channel Fast Inactivation. Neuron, 1999. 22:73-98.

41. Rojas CV, Neely A, Velasco-Loyden G, Palma V, Kukuljan M. Hyperkalemic periodic paralysis M1592V mutation modifies activation in human skeletal muscle Na+ channel. The American journal of physiology, 1999;276(1 Pt 1):C259-66.

42. Cummins T, Zhou J, Sigworth F, Ukomadu C, Stephan M, Ptáček L, Agnew W. Functional Consequences of a Na+ Channel Mutation Causing Hyperkalemic Periodic Paralysis. Neuron, 1993;10(4):667-78.

43. Cannon SC, Brown RH, Corey DP. A sodium channel defect in hyperkalemic periodic paralysis: potassium-induced failure of inactivation. Neuron, 1991 May 01;6(4):619-26.

44. Lehmann-Horn F, Kuther G, Ricker K, Grafe P, Ballanyi K, Rudel R. Adynamia episodica hereditaria with myotonia: a non-inactivating Na current and the effect of extracellular pH. Muscle Nerve, 1987 Aug 28;10:363-74.

45. Clausen T, Nielsen OB, Clausen JD, Pedersen TH, Hayward LJ. Na+,K+-pump stimulation improves contractility in isolated muscles of mice with hyperkalemic periodic paralysis. The Journal of General Physiology, 2011 Jul;138(1):117-30.

46. Pedersen TH, Clausen T, Nielsen OB. Loss of force induced by high extracellular [K+] in rat muscle: effect of temperature, lactic acid and beta2-agonist. The Journal of physiology, 2003 Aug 15;551(Pt 1):277-86.

47. Scott W, Stevens J, Binder Macleod SA. Human Skeletal Muscle Fiber Type Classifications, 2001. 81:1810-1816.

48. Schiaffino S. Myosin isoforms in mammalian skeletal muscle. Journal of Applied Physiology, 1994. 77:493-501.

49. Schiaffino S, Gorza L, Sartore S, Saggin L, Ausoni S, Vianello M, Gundersen K, Lømo T. Three myosin heavy chain isoforms in type 2 skeletal muscle fibres. Journal of muscle research and cell motility, 1989 Jul;10(3):197-205.

50. Bassel-Duby R. Signaling Pathways in Skeletal Muscle Remodeling - Annual Review of Biochemistry, 2006. 75(1):19.

51. Pette D, Staron RS. Myosin isoforms, muscle fiber types, and transitions. Microscopy research and technique. [Review]. 2000 Sep 15;50(6):500-9.

52. Bach L. Conversion of Red Muscle to Pale Muscle. Proceedings of the Society for Experimental; 1948. 67(3):268-269.

53. Salmons S, Vrbová G. The influence of activity on some contractile characteristics of mammalian fast and slow muscles. The Journal of physiology, 1969 Jun 01;201(3):535-49.

54. Conjard A, Peuker H, Pette D. Energy state and myosin heavy chain isoforms in single fibres of normal and transforming rabbit muscles. Pflügers Archiv : European journal of physiology, 1998 Oct 12;436(6):962-9.

55. Termin A, Staron R. Changes in myosin heavy chain isoforms during chronic low-frequency stimulation of rat fast hindlimb muscles - European Journal of Biochemistry 1989. 186:749-754.

56. Milton RL, Behforouz MA. Na channel density in extrajunctional sarcolemma of fast and slow twitch mouse skeletal muscle fibres: functional implications and plasticity after fast motoneuron transplantation on to a slow muscle. Journal of muscle research and cell motility, 1995 Aug 01;16(4):430-9.

57. Demirel H, Powers S, Naito H. Exercise-induced alterations in skeletal muscle myosin heavy chain phenotype: dose-response relationship. Journal of Applied Physiology, 1999. 86:1002-1008

58. Dolmetsch RE, Lewis RS, Goodnow CC, Healy JI. Differential activation of transcription factors induced by Ca2+ response amplitude and duration. Nature. [In Vitro]. 1997 May 24;386(6627):855-8.

59. Chin ER, Olson EN, Richardson JA, Yang Q, Humphries C, Shelton JM, Wu H, Zhu W, Bassel-Duby R, Williams RS. A calcineurin-dependent transcriptional pathway controls skeletal muscle fiber type. Genes & Development, 1998 Aug 15;12(16):2499-509.

60. Delling U, Tureckova J, Lim HW, De Windt LJ, Rotwein P, Molkentin JD. A calcineurin-NFATc3-dependent pathway regulates skeletal muscle differentiation and slow myosin heavy-chain expression. Molecular and cellular biology, 2000 Sep;20(17):6600-11.

61. Lin J, Wu H, Tarr PT, Zhang C-Y, Wu Z, Boss O, Michael LF, Puigserver P, Isotani E, Olson EN, Lowell BB, Bassel-Duby R, Spiegelman BM. Transcriptional co-activator PGC-1 alpha drives the formation of slow-twitch muscle fibres. Nature, 2002 Aug 15;418(6899):797-801.

62. Röckl K, Witczak C. Signaling mechanisms in skeletal muscle: Acute responses and chronic adaptations to exercise - Röckl - 2008 - IUBMB Life - Wiley Online Library. IUBMB life, 2008. 60(3)145-153.

63. Yan Z, Okutsu M, Akhtar Y. Regulation of exercise-induced fiber type transformation, mitochondrial biogenesis, and angiogenesis in skeletal muscle. Journal of Applied Physiology, 2011. 110:264-274.

64. Lupa MT, Krzemien DM, Schaller KL, Caldwell JH. Aggregation of sodium channels during development and maturation of the neuromuscular junction. J Neuroscience, 1993 Mar 1;13(3):1326-36.

65. Steel RT, JH. Principles and procedures of statistics. A biometrical approach. New York: McGraw-Hill; 1980.

66. Thabet M, Miki T, Seino S, Renaud JM. Treadmill running causes significant fiber damage in skeletal muscle of KATP channel-deficient mice. Physiol Genomics, 2005 Jul 14;22(2):204-12.

67. Banas K, Clow C, Jasmin B. The KATP channel Kir6.2 subunit content is higher in glycolytic than oxidative skeletal muscle fibers. American Journal of Physiology, 2011. 301:R916-R925

68. Mänttäri S, Träskbäck T, Järvilehto M. Sodium channel development changes the conduction velocity in skeletal muscle. Basic and Applied Myology, 2005 Feb 7;15(1):23-8.

69. Massett M, Berk B. Strain-dependent differences in responses to exercise training in inbred and hybrid mice. American Journal of Physiology-Regulatory Integrative and Comparative Physiology, 2005;288(4):R1006-R13.

70. Baar K, Wende A, Jones T, Marison M. Adaptations of skeletal muscle to exercise: rapid increase in the transcriptional coactivator PGC-1. The FASEB journal, 2002. 16:1879-1886

71. Fitts R, Booth F, Winder W. Skeletal muscle respiratory capacity, endurance, and glycogen utilization. American Journal of Physiology, 1975. 228(4):1029-1033.

72. Mondon CE, Dolkas CB, Sims C, Reaven GM. Spontaneous running activity in male rats: effect of age. 1985. 58(5)1553-1557.

73. Sprott RL, Eleftheriou BE. Open-Field Behavior in Aging Inbred Mice. Gerontology, 1974;20(3):155-62.

74. Andonian M, Fahim M. Effects of endurance exercise on the morphology of mouse neuromuscular junctions during ageing. Journal of neurocytology, 1987. 16:589-599.

75. Fahim M. Ultrastructural studies of young and old mouse neuromuscular junctions. Journal of neurocytology, 1982. 11:641-656.

76. Schefer V. Oxygen consumption in adult and aged C57BL/6J mice during acute treadmill exercise of different intensity. Experimental gerontology, 1996. 31(3):387-392.

77. Godt RE, Nosek TM. Changes of intracellular milieu with fatigue or hypoxia depress contraction of skinned rabbit skeletal and cardiac muscle. The Journal of physiology. [In Vitro]. 1989 Jun 01;412:155-80.

78. Cairns SP, Buller SJ, Loiselle DS, Renaud J-M. Changes of action potentials and force at lowered [Na+]o in mouse skeletal muscle: implications for fatigue. American Journal of Physiology- Cell Physiology. [In Vitro]. 2003 Nov 01;285(5):C1131-41.

79. Holloszy JO, Coyle EF. Adaptations of skeletal muscle to endurance exercise and their metabolic consequences. 1984. 55(4):831-838.

80. Agbulut O, Noirez P, Butler-Browne G. Specific isomyosin proportions in hyperexcitable and physiologically denervated mouse muscle. FEBS letters, 2004. 561:191-194.

81. Staunton L, Jockusch H, Wiegand C, Albrecht T, Ohlendieck K. Identification of secondary effects of hyperexcitability by proteomic profiling of myotonic mouse muscle. Molecular bioSystems, 2011;7(8):2480-9.

82. Ausoni S, Gorza L, Schiaffino S. Expression of myosin heavy chain isoforms in stimulated fast and slow rat muscles. The Journal of Neuroscience, 1990. 10(1):153-160.

83. Calabria E, Ciciliot S, Moretti I, Garcia M, Picard A, Dyar KA, Pallafacchina G, Tothova J, Schiaffino S, Murgia M, Rao A. NFAT Isoforms Control Activity-Dependent Muscle Fiber Type Specification. Proceedings of the National Academy of Sciences of the United States of America, 2009 Aug 11;106(32):13335-40.

84. Zhou J, Todorovic SM, Feero WG, Barany F, Conwit R, Hausmanowa-Petrusewicz I, Fidzianska A, Arahata K, Wessel HB, Sillen A, Marks HG, Hartlage P, Galloway G, Ricker K, Lehmann-Horn F, Hayakawa H, Hoffman EP, and Wang J. Molecular genetic and genetic correlations in sodium channelopathies: Lack of founder effect and evidence for a second gene. American Journal of Human Genetics, 1993 Jul 01;52(6):1074.

85. Subramony S. Exercise and rest in hyperkalemic periodic paralysis. Neurology, 1986. 36:173-177.

86. McManis P, Lambert E. The exercise test in periodic paralysis - McManis - 2004 - Muscle & Nerve - Wiley Online Library. Muscle; Nerve, 1986. 81(9):704-710.

APPENDIX 1

Chemicals used in experimental protocols.

Materials	Concentration	Diluent	Source
OCT compund	-	-	Sakura, Japan
Isopentane	100%	-	Sigma-Aldrich, Canada
Ethanol	100%	-	Fisher Scientific, Canada
Bovine Serum Albumin (BSA)	0.5% (w/v)	1X PBS	Sigma-Aldrich, Canada
Horse Serum	5% (w/v)	1X PBS	Sigma-Aldrich, Canada
10X Phosphate Buffered Saline (PBS)	1X	DD H2O	Fisher Scientific, Canada
Triton-X 100	0.3% (v/v)	1X PBS	J.T. Baker Chemical, USA
Fluorescent mounting medium	-	-	Dako, Canada
Buffered Neutral Formalin 10%	-	-	BDH, Canada
Hematoxylin	-	-	Shandon, USA
Eosin	-	-	Shandon, USA
HCL contentrate	100%	-	Fisher Scientific, Canada
Lithium Carbonate	-	-	Fisher Scientific, Canada
Toluene	-	-	Fisher Scientific, Canada
Permount mounting medium	-	-	Fisher Scientific, Canada

Materials	Concentration	Diluent	Source
TRIS	1 M	DD H2O	Invitrogen
NaCl	5 M	DD H2O	Fisher
EDTA	0.5 M	DD H2O	Sigma
SDS	10%	DD H2O	Sigma
PROTINASE K (PK)	10 mg/ml	DD H2O	Invitrogen
1:1 Phenol:CIA	-	-	Invitrogen
CIA	-	-	VWR
ISO-Propyl alcohol	-	-	Fisher
70% Ethanol	-	-	Fisher
Phusion Buffer/DMSO	-	-	NEB
DNAse-free H_2O	-	-	Fisher
NC1F	-	-	IDT
FC2R	-	-	IDT
Buffer#2/NSP1/BSA	-	-	NEB
Agarose	-	-	Cedarlane

Materials	Concentration	Diluent	Source
Na EDTA	-	-	Sigma
Boric Acid	-	-	EM Science
Ethidium Bromide	-	-	Sigma
DNA Loading Dye	-	-	Fermentas
100bp DNA Ladder	-	-	Fermentas